NACA

RESEARCH MEMORANDUM

STUDY OF EXIT PHASE OF FLIGHT OF A VERY HIGH ALTITUDE HYPERSONIC AIRPLANE BY MEANS OF A PILOT-CONTROLLED ANALOG COMPUTER

By Windsor L. Sherman, Stanley Faber,
and James B. Whitten

Langley Aeronautical Laboratory
Langley Field, Va.

NATIONAL ADVISORY COMMITTEE
FOR AERONAUTICS

WASHINGTON

March 4, 1958

NATIONAL ADVISORY COMMITTEE FOR AERONAUTICS

RESEARCH MEMORANDUM

STUDY OF EXIT PHASE OF FLIGHT OF A VERY HIGH ALTITUDE HYPERSONIC AIRPLANE BY MEANS OF A PILOT-CONTROLLED ANALOG COMPUTER

By Windsor L. Sherman, Stanley Faber, and James B. Whitten

SUMMARY

The effect of aerodynamic parameters on the ability of a pilot to control a hypersonic research airplane capable of flight at very high altitudes is studied by means of an analog computer. In this study, the airplane, which is a rocket-powered glide type, is flying a portion of the exit phase of a high-altitude trajectory that was selected so that the thrust cutoff occurs about halfway through the flight. In addition to aerodynamic effects, the influence of engine thrust misalinements, damping, and display information arrangement on the control task are considered.

The results, which are based on pilot opinion of the difficulty of the control task, are illustrated by time histories of angle of attack, angle of sideslip, and roll angle. The pilot attempted to hold these quantities at zero. In general, the findings of this investigation were that the basic airplane configuration used in this study was unflyable because of the extreme concentration and effort required to control the airplane, increased directional stability and additional damping about all three axes were necessary to make the basic airplane flyable, and, in addition, the arrangement of information in the pilot's display was found to have an important influence on the control task and the evaluation of the importance of aerodynamic parameters.

INTRODUCTION

The joint research-airplane program of the National Advisory Committee for Aeronautics, United States Air Force, and Department of the Navy was conceived and conducted to obtain flight data and to define

the operational problems associated with high-speed—high-altitude flight. It was decided to extend this program to include hypersonic airplanes capable of flight at very high altitudes. Preliminary wind-tunnel tests of proposed configurations revealed unusual magnitudes of and relationships between the stability derivatives. When these data were reviewed in light of the expected velocity, density, and altitude changes of the assumed flight plans, it was felt that customary stability and control criteria might not apply to these airplanes. Accordingly, a simulator study program was initiated in order to obtain some insight into the stability and control characteristics of this research airplane. These studies ranged from classical stability studies of the lateral and longitudinal responses to pilot-controlled studies of simulated flights such as reported herein. These pilot-controlled studies range from two-degree-of-freedom longitudinal simulations to five-degree-of-freedom simulations with Mach number and dynamic pressure programed to correspond to an assumed flight plan.

The aerodynamic data for a proposed research configuration were used as a starting point and then were modified as the study program progressed to obtain more general results. The configuration is a rocket-powered airplane of conventional design equipped with a horizontal tail that deflects in the conventional manner for pitch control and differentially for roll control.

In the simulator study of this report, the pilot's task was to fly the exit phase of an assumed high-altitude-flight plan. The exit phase was chosen because of the wide range of flight conditions over which the pilot must control the airplane and also because burnout occurs during the climb and can introduce violent trim changes. A five-degree-of-freedom simulation was used with the velocity and dynamic pressure programed to agree with that of the assumed flight plan.

The conclusions of this study are based on the opinions of the NACA pilots who made the simulated flights. Specifically, the pilots attempted to evaluate the flyability of the airplane represented on the simulator in the light of their experience with existing airplanes. Where possible, time histories of the flights are used to illustrate the pilot's opinion.

This report includes an appendix by Robert E. Andrews, of the Langley Laboratory, which presents a discussion of the analog simulator programing.

SYMBOLS

h	altitude
q_d	dynamic pressure

[redacted]

I_x, I_y, I_z moments of inertia about the X-, Y-, Z-axes

E_{m_V} engine thrust misalinement, vertical

E_{m_H} engine thrust misalinement, horizontal

ψ yaw angle or heading angle

ϕ Euler roll angle

θ Euler pitch angle

m mass of airplane

M Mach number

α angle of attack

β sideslip angle

Δ incremental value from initial condition (for example, $\Delta\theta$ indicates increment in pitch angle)

C_l rolling-moment coefficient, $\frac{\text{Rolling moment}}{q_d S b}$

C_n yawing-moment coefficient, $\frac{\text{Yawing moment}}{q_d S b}$

C_m pitching-moment coefficient, $\frac{\text{Pitching moment}}{q_d S \bar{c}}$

C_{m_o} pitching-moment coefficient at zero angle of attack

δ_h horizontal-tail deflection for pitch control

δ_h' differential horizontal-tail deflection for roll control

δ_v vertical-tail deflection for yaw control

$C_{m_\alpha} = \frac{\partial C_m}{\partial \alpha}$

[redacted]

$$C_{m_q} = \frac{\partial C_m}{\partial \frac{q\bar{c}}{2V}}$$

$$C_{m_{\dot{\alpha}}} = \frac{\partial C_m}{\partial \frac{\dot{\alpha}\bar{c}}{2V}}$$

$$C_{m_{\delta_h}} = \frac{\partial C_m}{\partial \delta_h}$$

$$C_{l_\beta} = \frac{\partial C_l}{\partial \beta}$$

$$C_{l_p} = \frac{\partial C_l}{\partial \frac{pb}{2V}}$$

$$C_{l_{\delta_{h'}}} = \frac{\partial C_l}{\partial \delta_{h'}}$$

$$C_{l_{\delta_v}} = \frac{\partial C_l}{\partial \delta_v}$$

$$C_{n_r} = \frac{\partial C_n}{\partial \frac{rb}{2V}}$$

$$C_{n_\beta} = \frac{\partial C_n}{\partial \beta}$$

$$C_{n_{\delta_{h'}}} = \frac{\partial C_n}{\partial \delta_{h'}}$$

$$C_{n_{\delta_v}} = \frac{\partial C_n}{\partial \delta_v}$$

C_Y side-force coefficient, $\frac{\text{Side force}}{q_d S}$

$C_{Y_\beta} = \frac{\partial C_Y}{\partial \beta}$

$C_{n_p} = \frac{\partial C_n}{\partial \frac{pb}{2V}}$

$C_{l_r} = \frac{\partial C_l}{\partial \frac{rb}{2V}}$

b	span, 22.36 ft
S	wing area, 200 sq ft
$\bar{c}$	mean aerodynamic chord, 10.27 ft
$C_{Y_{\delta_v}} = \frac{\partial C_Y}{\partial \delta_v}$	
C_L	lift coefficient, $\frac{\text{Lift}}{q_d S}$
$C_{L_\alpha} = \frac{\partial C_L}{\partial \alpha}$	
p, q, r	airplane angular velocities about the x, y, z body axes
u, v, w	airplane line velocities along the x, y, z body axes
l_i, m_i, n_i	direction cosines relating the airplane body axes and space axes ($i = 1, 2, 3$)
g	acceleration due to gravity, 32.17 ft/sec^2
V	total velocity, $\sqrt{u^2 + v^2 + w^2}$
K_1	roll-damper gain
K_2	pitch-damper gain
K_3	yaw-damper gain

[redacted]

δ_L	deflection of left side of horizontal tail
δ_R	deflection of right side of horizontal tail
δ_{S_ϕ}	roll control signal from control stick
δ_{S_θ}	pitch control signal from control stick
δ_{p_ψ}	yaw control signal from rudder pedals
W_H	oscilloscope display signal for horizontal component of wing
W_V	oscilloscope display signal for vertical component of wing
T_H	oscilloscope display signal for horizontal component of tail
T_V	oscilloscope display signal for vertical component of tail
ω	oscilloscope display sweep frequency, 300 cps
I.C.	initial condition

STATEMENT OF THE PROBLEM AND DISCUSSION OF SIMULATION

The objective of this study was to evaluate in a qualitative manner the effect of the aerodynamic characteristics of the proposed research configuration with respect to a pilot's ability to perform a specific control task during a part of the exit phase, which includes thrust cut-off, of a typical high-altitude-flight plan. In addition, it was desired to determine the trends airplane characteristics should take to ease the control tasks and to determine the effect of information display on the control task. The flight plan selected was essentially a ballistic trajectory and, therefore, the control task assigned the pilot was to maintain the angles of attack, roll, yaw, and sideslip at zero throughcut the flight. The details of the simulation, including the equations used, are presented in the appendix. The simulation is summarized in the following paragraphs.

Figure 1 is a simplified block diagram of the simulation that shows information flow. Reference to it should be of help in following the discussion of the simulation.

The assumed variations of Mach number, dynamic pressure, and altitude used in this study are presented in figure 2. Engine cutoff (burnout) has been arbitrarily set at 83 seconds. The part of this figure between the vertical-dashed lines, that portion from 55 seconds to 105 seconds, is the portion of the flight plan over which this study was conducted. The data presented in figure 2 show the wide range of flight conditions over which the pilot must control the airplane. The basic parameters, Mach number and dynamic pressure, vary from 3.2 and 350 pounds per square foot to 5.5 and 20 pounds per square foot, respectively, during the simulated flight. These variations indicate that the basic stability characteristics of the airplane are also subject to wide variation. As indicated in figure 2, burnout occurs approximately 28 seconds after the start of the problem.

In this study, in order to simplify the analog, it was assumed that the Mach number and dynamic-pressure variations would be those of the calculated flight plan - that is, they would be unaffected by any of the random motions occurring in the simulator flights. This assumption permitted the velocity, Mach number, and dynamic pressure to be expressed as functions of the flight time. The airplane was represented as a five-degree-of-freedom system with time-varying coefficients (those depending on Mach number and dynamic pressure). These equations were referred to the principal body axes. As the inclination of the principal axis is very small, the effect of this inclination was considered negligible. Programed variations of mass and inertia were also used to account for the large change in these quantities due to rocket burning, and the variations in these parameters assumed for this study are presented in figure 3.

The aerodynamic parameters used were obtained from the unpublished results of wind-tunnel tests of an advanced research configuration. The static stability derivatives were programed as functions of Mach number and were assumed to remain constant with angle of attack and angle of sideslip. These variations are shown in figures 4(a) to 4(f). In figure 4(a) the curve labeled C_{n_β} is the basic C_{n_β} of the airplane and that labeled $C_{n_{\beta_A}}$ represents the maximum value of C_{n_β} used. Results will be reported for both C_{n_β} and $C_{n_{\beta_A}}$. In figure 4(b), three curves are presented for C_{l_β}. The center curve is the basic C_{l_β} for the airplane and the other two curves bracket the variations assumed in the effective-dihedral parameter. The assumption of constant derivatives with angle of attack is very good; wind-tunnel results show these parameters to be constant from 0 to 9°. Since the assumed flight plan called for zero angle of attack, it was felt that, if the range of angle of attack where the stability derivatives became nonlinear functions of

[redacted]

angle of attack were entered, it would be only momentarily. Actual simulator runs showed this to be true, with α rarely exceeding 10°. The assumption of constant derivatives with angle of sideslip was good for small angles of sideslip - that is, to the 5° maximum of the wind-tunnel tests. Since successful flights rarely exceeded this value of sideslip, the assumption is considered satisfactory for these simulator tests. Although no data were available for the rotary derivatives, provisions were made in the setup for their eventual inclusion. The control-surface-effectiveness coefficients were not programed with Mach number since data were available only at $M = 3.5$. These data are presented in table I. The actual moments and forces produced by the surfaces were not constant, however, due to the programed changes in the dynamic pressure.

As noted previously, rocket burnout occurs during the simulator flight. Early rocket airplanes, such as the Bell X-1A and Bell X-2 airplanes, have been troubled to a minor degree by the trim changes at burnout caused by thrust misalinement suddenly reducing to zero. Since the proposed thrust is roughly four times that of the Bell X-2, even more trouble could be expected. In order to determine these effects, engine thrust misalinements were included as constant moments in the yawing- and pitching-moment equations. These moments were calculated from data given in the engine progress reports and engine specifications and were found to have a maximum value of about 5,000 foot-pounds.

The pilot's control station consisted of a seat, control stick, and rudder pedals together with an information display (instrument panel). A photograph of this station is shown as figure 5. When in use, the station was enclosed in a canvas screen so that the pilot would not be distracted. The stick and pedal feel forces were supplied by simple springs and were, therefore, independent of Mach number or dynamic pressure. Table II summarizes the stick and pedal forces and travels and the attendant control-surface deflections. It should be pointed out that in the opinion of the test pilots the forces and moments shown in table II do not represent good control harmony. Some runs were made with better harmony after the investigation had been completed, and it was found that the difference in control harmony did not appreciably affect the results.

The information display consisted of three tightly grouped cathode-ray tubes (fig. 5). This display was developed after preliminary tests indicated a need for rapid scanning by the pilot. The details of the information display are shown in figure 6. The center cathode-ray tube presented the angle of attack α, the angle of sideslip β, and the roll angle ϕ, while the upper scope presented heading angle ψ and the left one presented pitch attitude θ. Hereinafter, this display is referred to as the β-ϕ display. The marker used on the center scope was an inverted T which may be thought of as the rear view of an airplane.

This marker displaced vertically to present α and horizontally to show β and rotated about its own axis to show ϕ. The scales for α and β were approximately 0.1 radian per inch. Negative sideslip was to the right to make the display compatible with flight. For the auxiliary scopes, the heading marker moved horizontally and the pitch marker moved vertically, both approximately 0.4 radian per inch.

The β-ϕ display was used for most of the investigation. However, some tests were made with a display more akin to standard flight instruments. This display was called the attitude display and presented pitch attitude θ, heading angle ψ, and roll angle ϕ on the center scope. The angles of attack and sideslip were on the auxiliary scopes. The scales for the attitude display were the same as those used on the β-ϕ display.

The pilot's display of roll attitude was set up for a moving airplane rather than the moving horizon that is used in most flight instruments. The use of the moving airplane was based on previous experience at the Langley Laboratory and on the results of reference 1, both of which indicated that, on simulators which do not move the pilot, the moving airplane is the preferred type of display or roll attitude.

Since the angular velocities of the airplane are computed in body axes, which are a rotating axes system, it was necessary to transfer these variables to space axes for the display. Equations (9) to (11) of the appendix were used to make the conversion.

A warning light which came on 3 seconds before thrust cutoff (burncut) was included in the display. This light provided the pilot with some anticipation of the trim changes which occur at thrust cutoff.

RESULTS AND DISCUSSION

Preliminary Analysis

Analytical investigation.- The lateral and longitudinal stability of the airplane was investigated by use of the three-degree-of-freedom stability equations at several points along the selected trajectory. These calculations showed that the basic airplane was always laterally unstable and that it had good longitudinal stability at the lower altitude flight conditions and had approximately neutral static stability at the high-altitude flight conditions. The addition of estimated rotary derivatives increased the stability at the low altitudes and delayed the onset of instability to moderate altitudes. The effect of the rotary derivatives at high altitude was negligible.

The effects of stability augmentation were approximated by adding appropriate increments in the rotary derivatives C_{n_r} and C_{l_p} to the lateral equations and C_{m_q} to the longitudinal equations. The addition of either C_{n_r} and C_{l_p} alone had little or no effect on the Dutch roll mode. However, the addition of both resulted in large improvements in stability. In the longitudinal equations, the addition of C_{m_q} produced good stability throughout the flight realm. The values of each of these parameters required to give good stability are summarized for the flight conditions at burnout as follows:

$$\Delta C_{m_q} = -221.15$$

$$\Delta C_{n_r} = -42.3$$

$$\Delta C_{l_p} = -2.602$$

These values give a roll damping of $T_{1/2} = 0.5$ second, Dutch roll damping of $T_{1/2} = 0.9$ second, and pitch damping of $T_{1/2} = 0.75$ second at a flight time of 28 seconds, the time of thrust cutoff. These values of the damping derivatives were used to give an indication of the damping required on the simulator.

Constant Mach number simulator studies.- As part of a pilot familiarization program prior to making the trajectory flights, several flights were made at constant Mach number and altitudes. These flights were made at altitudes of 84,000 and 180,000 feet, the end points of the trajectory. In these flights the pilots attempted to evaluate the stability and control characteristics during maneuvers. These maneuvers were generally a return to straight and level flight from initial disturbances in α and β and constant altitude turns with a bank angle of 45°. At the low-altitude flight condition the pilots felt that the basic airplane was extremely difficult to control and that to avoid losing control all maneuvers had to be very slow and deliberate. Three-axis damping equivalent to 50 percent of the damping required for the linear analyses improved the handling characteristics under the aforementioned conditions. During these simulated piloting tasks the pilots complained of apparent low control power in yaw and roll control. This apparent loss of control power to the pilot results because the dampers are using so much of the available control-surface deflection to correct disturbances that, when the pilot moves the controls, the airplane does not respond to his input. Thus, as the magnitude of the artificial damping is increased, the apparent control power of the surfaces, as

perceived by the pilot, decreases. At high altitude the response of the basic airplane was so slow that the pilot had no difficulty in maintaining control.

Trajectory Flights

The procedure used in these flights was to have the pilot trim the airplane at a flight-path angle of 31.5° as called for by the flight plan. When trim conditions had been established, the pilot flew the airplane over the programed portion of the flight plan. In these flights the pilot's task was to hold α, β, ϕ, and the angular velocities to zero. Sufficient practice and repeat flights were made so that the pilots were completely familiar with the simulator characteristics.

In interpreting the results of the investigation made during the trajectory flights, it should be remembered that, as the airplane accelerates and climbs, the airplane becomes less stable and the air density decreases. Both these effects increase the periods of the airplane's oscillation. The longer periods tend to ease the pilot's control task as long as directional instability does not occur. However, a high degree of alertness must be maintained as motions develop very slowly at these high altitudes and by the time the pilot detects a deviation from the desired condition it may be too late for corrective action.

The first trajectory flight was made with the basic airplane and without disturbances - that is, there were no engine thrust misalinements and no external disturbances were used with respect to the airplane or pilot. The pilot was able to control the simulator and to complete the flight plan. However, the pilot stated that he had great difficulty in controlling the simulator and, because of the extreme concentration required, considered airplanes with these characteristics unflyable. The recorded motions of the airplane and of the control stick and pedals did not show undue difficulty. In order to demonstrate this concentration level, flights were made in which an additional work load was given the pilot. One additional work load imposed was the distraction of the pilot to tasks other than flying. This was simulated by intercepting the pilot's view of the display for not more than 5 seconds at different times during the flight. Another additional work load was the control of engine thrust asymmetries during burning flight and resultant trim changes which occur at thrust cutoff. As the engine thrust asymmetries were constant, the pilot, as the altitude increases, must continuously increase his control deflections in order to correct the out-of-trim conditions. Figure 7(a) shows the effect of the distraction and of a vertical thrust misalinement on the pilot's ability to maintain control of the airplane. When the pilot's attention to the control task was

momentarily diverted, he lost control of the airplane. As indicated by the solid curve in figure 7(a), the addition of a vertical thrust misalinement apparently caused the pilot no additional difficulty over and above those associated with the basic airplane. However, when a lateral thrust misalinement was added, figure 7(b), the pilot lost control of the airplane before burnout. This result substantiates the results of the linear analysis and constant Mach number flights which indicated that the airplane was more sensitive to lateral disturbances.

Effect of directional stability.- One possible cause of the difficulty experienced by the pilots can be seen in figure 4(a), which presents the variations with Mach number of the static lateral stability parameter C_{n_β}. Shown are the basic wind-tunnel data and also the other variations used in this study. The basic data show that at a Mach number of 4.4 the airplane becomes directionally unstable. This trend in C_{n_β} accounts for the buildup in sideslip noted when the pilot was distracted. The rolling and pitching motions noted were due to the high ϕ/β ratio and the inertia coupling of the airplane at these flight conditions. An increased C_{n_β}, shown in figure 4(a) as $C_{n_{\beta_A}}$, which made the configuration stable throughout the Mach number range considered was also tested. With this increase in C_{n_β} the pilot was able to maintain control over the programed part of the trajectory, even when momentarily distracted or when thrust misalinements were included. (Compare figs. 7 and 8.) It must be noted, however, that many practice flights were required before successful flights were obtained with any consistency. Although it was possible to maintain control, the pilots were of the opinion that an airplane with the characteristics simulated was still unflyable.

Damping studies.- As indicated by both the linear analysis and the simulator flights, additional damping was required. Investigations were made of both augmentation as obtained from control-surface deflections and as increments in the rotary derivatives C_{n_r}, C_{l_p}, and C_{m_q}. In the control-surface-augmentation cases, the assumption was made that the surface would deflect proportional to the angular velocity through a perfect servo system. For similar amounts of damping, no difference was found between the two types of augmentation; this indicated that the effects of the moments introduced by the cross-control terms $C_{n_{\delta_h}}$ and $C_{l_{\delta_v}}$ were small. This result is for the restricted condition of three-axis damping and small angle of attack. If either of these conditions is not met, the effects of these moments may become very important as they do when the yaw damper is not used.

[redacted]

The amount of damping was systematically increased until the pilot felt the airplane possessed the minimum stability to fly the trajectory. As a starting point, damping equivalent to the estimated rotary derivatives was tested. This amount of damping had no noticeable effect on the airplane motions or the control task.

In the pilot's opinion, sufficient damping was obtained with about one-half of the reference values determined by linear analysis. Figure 9 compares a flight with this amount of three-axis damping and a similar flight without damping. Thrust misalinements were included in both cases. It should be pointed out that this amount of damping was sufficient during the climbing trajectory in which the pilot was not concerned with other flight tasks and could concentrate his entire effort on the control tasks. Also, in the simulator, the control system was almost perfect - that is, no slop or lags - and, further, the pilot was not subject to any random forces or motions. Thus, because of these differences between simulated and actual flight and because the type of display may have an influence on the amount of damping required, the magnitudes of damping required for good stability and control determined in this study are only qualitative and based on pilot's opinion.

Further increases in augmentation were made until the damping was equivalent to reference values established by the linear analysis. The pilots preferred this damping to lesser amounts but with reservations because of the adverse effect of damping on the response of the airplane to the pilot's control inputs. This increase in damping did not affect the airplane motions to any noticeable extent, the added augmentation merely reducing the work required of the pilot.

A brief study was made of the effect of the individual dampers on the control tasks. The following table shows the combinations tried and the pilot's opinion reduced to a numerical scale, 4 being the most acceptable and 0 being unacceptable:

Case	Damper	Pilot's rating
A	Roll yaw pitch	4
B	Roll yaw	2, pitch oscillation bothersome
C	Roll pitch	0, Dutch roll less stable
D	Yaw pitch	3
E	Pitch	2, difficult to control yaw oscillations

In this part of the damping study both favorable and unfavorable yawing moments due to roll control were used. (See table I.)

While three-axis damping was the preferred condition, the pilot felt the omission of the roll damper was least critical. In addition, the pilot thought that if the yaw damper failed the roll damper should be shut off immediately. It was found that the roll damper caused the Dutch roll mode to become considerably less stable when the yawing moment due to the rolling tail deflection was favorable. In this case, the action of the roll control surfaces to damp the rolling motion caused a negative C_{n_p} to be introduced which resulted in a deterioration of the Dutch roll damping. When a yaw damper was used, it counteracted the unfavorable (negative) C_{n_p} effect and the Dutch roll mode was found satisfactory by the pilot. These results indicate that, when an airplane has low inherent damping and a favorable yawing moment from the roll control surfaces, the roll damper and rudder should be interconnected so that the rudder deflects with the ailerons to compensate for the unfavorable C_{n_p} introduced by use of the ailerons to oppose the roll.

Inasmuch as the aerodynamic characteristics of this airplane vary with angle of attack, the results of the damping study are limited to the small perturbations about zero angle of attack for the aerodynamic characteristics cited in table I and figure 4.

Effect of dihedral parameter C_{l_β}.- Another cause of the control difficulty experienced by the pilot was the high ratio of roll to sideslip of the configuration. A contribution to this ratio is the rolling moment due to sideslip C_{l_β}. Figure 4(b) presents the variation with Mach number of this parameter for the basic configuration of the tests. Also shown are the extreme negative and positive variations studied. The pilots' comments on the effects of C_{l_β} can be summarized as follows: Increasing C_{l_β} from zero in either the negative or positive direction increased the difficulty of controlling the airplane; however, for the range of values of C_{l_β} used the effect of this parameter on the control task was of secondary importance.

Control-effectiveness studies.- Because of the lack of comprehensive wind-tunnel data at the time of programing, the control-surface-effectiveness coefficients were assumed to be constant with Mach number. Information now available indicates that the ratios used were fair average values with the low value at $M = 3.2$ and the high value at $M = 5.5$.

The direct moments - that is, the moments caused by $C_{l_{\delta_{h'}}}$, $C_{m_{\delta_h}}$, and $C_{n_{\delta_v}}$ - gave adequate control power at the low-altitude part of the flight; however, at the high-altitude high Mach number range, the pilot felt that the roll and yaw control power was very low. The pitching moment provided by the horizontal-tail coefficient $C_{m_{\delta_h}}$ proved to be adequate for the task of maintaining zero angle of attack through the part of the flight that was simulated.

The effects of cross-control moments, yaw due to the roll control and roll due to the rudder, provided by the coefficients $C_{n_{\delta_{h'}}}$ and $C_{l_{\delta_v}}$ were also evaluated. The rolling moment due to the rudder was larger than the rolling moment due to the rolling tail, and this proved quite objectionable to the pilot until new coordination techniques were learned. After the learning period the pilots considered the $C_{l_{\delta_v}}$ effect on the control task to be secondary to the lack of directional stability and damping, although they indicated that a near-zero value of this parameter was preferable. The effect of yawing moment due to roll control was not as obvious, the pilot noticing little or no effect of magnitude changes and no difference between favorable and unfavorable values of $C_{n_{\delta_{h'}}}$. The lack of effect of $C_{n_{\delta_{h'}}}$ on pilot opinion is caused by the fact that the contribution of $C_{n_{\delta_{h'}}}$ to the total yawing moment is small as compared with the contribution of the other parameters. However, as previously pointed out, a favorable $C_{n_{\delta_{h'}}}$ tends to make the Dutch roll mode less stable when yaw damping is omitted from the system.

The cross-control-effectiveness parameters $C_{n_{\delta_{h'}}}$ and $C_{l_{\delta_v}}$ have an effect on the ability of the rudder to produce a yawing moment. When a yawing moment is applied to the system and it is desired to maintain zero sideslip and wings level, the rudder deflection δ_v to cancel the applied moment is given by

$$\delta_v \left(C_{n_{\delta_v}} - \frac{C_{n_{\delta_{h'}}} C_{l_{\delta_v}}}{C_{l_{\delta_{h'}}}} \right) = \frac{N}{qSb}$$

[redacted]

The term in parentheses can be considered the effective yawing-moment coefficient due to vertical-tail deflection. Thus, when $C_{n_{\delta_{h'}}}$ and $C_{l_{\delta_v}}$ have the same sign, the effective $C_{n_{\delta_v}}$ is smaller than when $C_{n_{\delta_{h'}}}$ and $C_{l_{\delta_v}}$ have opposite signs and, thus, more rudder deflection is required to cancel the applied yawing moment. This condition can become quite serious when the pilot is trying to control engine thrust asymmetries or large-amplitude lateral oscillations. Figure 10 is an illustration of this effect when the pilot is trying to trim engine thrust asymmetries. In this case the rudder power becomes inadequate just before burnout and the pilot almost immediately loses control of the airplane. In this flight the physical stop on the pilot's control was 5° instead of the 6° indicated in table II. This discrepancy was caused by centering difficulties in the rudder pedals.

Display studies.- As previously noted, two different displays were used during this investigation. One of these was the β-ϕ display used for the study up to this point, in which α, β, and ϕ were on a single inverted T marker on the center oscilloscope and θ and ψ were on auxiliary oscilloscopes. The second was the attitude display which presented θ, ψ, and ϕ on the center oscilloscope and α and β on the auxiliary oscilloscopes. Comparison flights of the displays showed that the pilot when using the attitude display, found the control task to be more difficult than when using the β-ϕ display. For instance, the effective-dihedral parameter which the pilots felt to be of secondary importance with the β-ϕ display was found to be critically important with the attitude display. Figure 11 compares the motions of the airplane for the two information displays. These flights were made with the basic airplane modified by increasing C_{n_β} and C_{l_β} to the maximum stable values of figure 4 and rotary derivatives with values of $C_{l_p} = -0.2601$, $C_{m_q} = -11.05$, and $C_{n_r} = -0.873$. No auxilary damping was supplied. When the attitude display was used, the airplane motions have large amplitudes and the pilot loses control of the airplane just before engine thrust cutoff. When the β-ϕ display was used, the motions have a much smaller amplitude although the frequency is about the same and the pilot was able to maintain control of the airplane throughout the flight.

The major difference between the two displays is in the presentation of information. The airplane studied is characterized by a high ϕ/β ratio and low aileron and rudder power. These characteristics require the pilot to maintain very close control over and to coordinate closely the β-ϕ motions of the airplane. Thus, the display that presents ϕ and β by the motion of a single marker eased the pilot's task by

reducing the scanning and data-assimilation time with respect to the more conventional attitude display. This reduction of scanning and data-assimilation time was further decreased by including the α indicator, the other critical control parameter, on the same marker.

This display investigation was limited to the climbing phase of a high-altitude flight plan where the specific control task was to hold α, β, and ϕ to 0. For conditions studied, data arrangement had a large effect on the difficulty of the control task. This result is corroborated by the simulator studies of an entirely different control task reported in reference 2.

Since other flight conditions will require different control tasks, further investigations should be made, including flight tests, before a final display arrangement for this project is evolved.

CONCLUDING REMARKS

The following conclusions may be drawn relative to the stability and control problems of a proposed research configuration during the exit phase of a high-altitude trajectory. These conclusions are based on pilot-controlled simulator studies of the airplane.

The proposed configuration was considered by the pilots to be unflyable because of the extreme concentration and mental effort required to maintain control. It was the pilots' opinions that directional stability and increased damping about all three axes were required before the airplane would attain a minimum stability for safe flying of the programed part of the trajectory. The investigation of the effective dihedral showed that this parameter had only a secondary influence on the control task when the β-ϕ display was used, whereas it had a primary influence when a more conventional attitude display was used.

The investigation of the effect of individual dampers on the control task indicated that the roll damper was the least critical. In addition, if the derivative of yawing moment due to the roll control is favorable and the yaw damper fails, the roll damper should be cut off immediately. The pitch damper, while not critical from a safety aspect, damped an oscillation that was bothersome to the pilot and in doing so eased the control task.

The pilots felt that the cross-control-effectiveness coefficients $C_{l_{\delta_v}}$ and $C_{n_{\delta_h}}$ should be kept as small as possible to ease the control task.

[redacted]

As a result of a limited display investigation it was concluded that instrument data arrangement can have an important effect on the control task and that for the tests reported herein the display combining together information for angles of attack, sideslip, and roll was desirable. It is suggested that further tests, including flight tests, be made to determine the instrument arrangement suitable for the entire flight plan of the airplane.

Langley Aeronautical Laboratory,
National Advisory Committee for Aeronautics,
Langley Field, Va., November 5, 1957.

REFERENCES

1. Anon.: Pilot Performance With Two Different Attitude Displays. AD No. 82868 (Contract Nonr 1076(00), Dunlap and Associates, Inc.,) Armed Services Tech. Information Agency, Doc. Service Center (Dayton, Ohic), July 1955.

2. Roscoe, S. N.: Data Presentation and Control Devices. Proc. Symposium on Frontiers of Man-Controlled Flight, Heinz Haber, ed., Inst. Transp. and Traffic Eng., Univ. of California, Los Angeles, 1953, pp. 70-74.

APPENDIX

THE ANALOG SIMULATOR PROGRAMING

By Robert E. Andrews

INTRODUCTION

This appendix presents the equations of motion which were simulated and a description of the mock cockpit. Also presented is a discussion of the difficulties encountered along with some of the checks performed to verify the simulator results. A complete schematic diagram of the analog simulation is shown in figure 12.

REPRESENTATION OF THE AIRPLANE

The airplane was represented by the five-degree-of-freedom equations with time-varying coefficients. The equations were written about the principal body axes and are as follows:

$$I_x\dot{p} = (I_y - I_z)qr + q_d Sb\left[C_{l_\beta}\beta + C_{l_{\delta_{h'}}}(\delta_R - \delta_L) + C_{l_{\delta_v}}\delta_v + \frac{b}{2V}\left(C_{l_p}p + C_{l_r}r\right)\right] \quad (1)$$

$$I_y\dot{q} = (I_z - I_x)pr + q_d S\bar{c}\left[C_{m_o} + C_{m_\alpha}\alpha + \frac{1}{2}C_{m_{\delta_h}}(\delta_R + \delta_L) + \frac{\bar{c}}{2V}\left(C_{m_q}q + C_{m_{\dot{\alpha}}}\dot{\alpha}\right)\right] + E_{M_V} \quad (2)$$

$$I_z\dot{r} = (I_x - I_y)pq + q_d Sb\left[C_{n_\beta}\beta + C_{n_{\delta_v}}\delta_v + C_{n_{\delta_{h'}}}(\delta_R - \delta_L) + \frac{b}{2V}\left(C_{n_r}r + C_{n_p}p\right)\right] + E_{M_H} \quad (3)$$

$$\dot{\beta} = -r + \alpha p + \frac{1}{V}\left[gm_3 - \dot{V}\beta + \frac{q_d S}{m}\left(C_{y_\beta}\beta + C_{y_{\delta_v}}\delta_v\right)\right] \quad (4)$$

$$\dot{\alpha} = q - p\beta + \frac{1}{V}\left[gn_3 - \dot{V}\alpha - \frac{q_d S}{m} C_{L_\alpha}\alpha\right] \tag{5}$$

The coefficients of these equations, which are functions of the Mach number and hence the flight time, are presented in table III. These expressions were obtained by fitting polynomials to the data presented in figures 2 to 4.

It was necessary to compute the direction cosines l_3, m_3, and n_3 so that the gravity forces could be properly included in the airplane representation. The following equations were used

$$l_3 = l_{3_0} + \int_0^t \left(m_3 r - n_3 q\right) dt \tag{6}$$

$$m_3 = m_{3_0} + \int_0^t \left(n_3 p - l_3 r\right) dt \tag{7}$$

$$n_3 = n_{3_0} + \int_0^t \left(l_3 q - m_3 p\right) dt \tag{8}$$

where $l_{3_0} = -\sin\theta_0$, $m_{3_0} = \sin\phi_0 \cos\theta_0$, and $n_{3_0} = \cos\phi_0 \cos\theta_0$.

PILOT'S DISPLAY AND METHOD OF CONTROL

The pilot's control station contained oscilloscopes to display the roll angle, sideslip angle, angle of attack, heading angle, and pitch-attitude angle. It also contained a conventional center control stick and rudder pedals. Figure 5 is a photograph of the control station.

Two different display combinations were used during this investigation. The same information was displayed in each but the location was different. The information was displayed on a 5-inch dual-beam oscilloscope in the form of an inverted T which rotated about its own axis and also translated horizontally and vertically. Two rectangular oscilloscopes, each 3 by $1\frac{1}{2}$ inches were arranged to show their displays through a mirror. One was mounted in a vertical position to the left of the main oscilloscope and the other was mounted horizontally above the main scope.

[redacted]

The first display combination, called the β-ϕ display, presented angles of attack, sideslip, and roll on the center oscilloscope and the pitch-attitude and heading angles on the left auxiliary and top auxiliary oscilloscopes, respectively. The inverted T rotates through an angle equal to the roll angle of the airplane, clockwise for positive angles. The angle of attack translates the T vertically, upward for positive angles, while the angle of sideslip translates the T horizontally, to the left for positive sideslip. The display on the left auxiliary oscilloscope presents a horizontal line which translates vertically with the pitch-attitude angle, upward for positive angles. The top auxiliary oscilloscope presents a vertical line which translates horizontally with the heading angle, to the right for positive angles.

The second display combination, called the attitude display, presents the roll angle, heading angle, and pitch-attitude angle on the main oscilloscope with angle of attack and angle of sideslip presented on the side and top auxiliary oscilloscopes, respectively.

The scales for angles of attack and sideslip were approximately 0.1 radian per inch for each display. The pitch-attitude and heading scales were approximately 0.4 radian per inch for both displays.

The angles presented in the display give the pilot the necessary information for orientation with respect to space as well as with respect to flight path. The Euler angles ϕ, θ, and ψ give the bank angle, pitch-attitude angle, and heading angle, respectively, with reference to space. The Euler angle equations have been simplified by setting $\sin\theta$ equal to zero and $\cos\theta$ equal to unity. These equations are

$$\phi = \phi_o + \int_0^t p \, dt \tag{9}$$

$$\theta = \theta_o + \int_0^t (q \cos\phi - r \sin\phi)dt \tag{10}$$

$$\psi = \psi_o + \int_0^t (r \cos\phi + q \sin\phi)dt \tag{11}$$

where $\phi_o = \psi_o = 0$ and $\theta_o = 31.5^\circ$.

The inverted T was generated by using a dual-beam oscilloscope with one beam generating the wing and the other beam the tail. For the wing

[redacted]

a sine wave was amplitude-modulated by resolving it by the sine and cosine of the roll angle ϕ, adding the translating voltage (α, β, θ, or ψ) to it, and connecting them to the horizontal and vertical plate of the first beam. The tail was generated similarly except that a rectified sine wave was used. For the β-ϕ display the four inputs to the oscilloscope were

$$W_V = \alpha + A \sin \omega t \sin \phi \tag{12}$$

$$W_H = -\beta - A \sin \omega t \cos \phi \tag{13}$$

$$T_V = \alpha - B \sin \omega t \cos \phi \tag{14}$$

$$T_H = -\beta - B \sin \omega t \sin \phi \tag{15}$$

where W_V and W_H are the signals applied to the vertical and horizontal plates of the beam producing the wing and T_V and T_H are signals applied to the tail beam. B sin ωt is the rectified signal from A sin ωt. The details of this setup are shown in the schematic arrangement in figure 12.

The pilot's controls were a conventional center position stick and rudder pedals to provide aerodynamic controls. Roll control was obtained by the differential deflection of the horizontal tail; thus, it was necessary to combine pitch and roll commands in the horizontal-tail surface deflections. This was done by computing separate deflections for the right and left sections of the horizontal tail by using the following equations:

$$\delta_R = \frac{1}{2}\delta_1 + \delta_2 - K_1 p + K_2 q \tag{16}$$

$$\delta_L = -\frac{1}{2}\delta_1 + \delta_2 + K_1 p + K_2 q \tag{17}$$

Heading control was obtained by an all-movable vertical surface, and the control deflection is given by

$$\delta_V = \delta_3 + K_3 r \tag{18}$$

[redacted]

Artificial damping is supplied to the airplane by feeding signals proportional to the angular velocity to the control surfaces. The terms K_1p, K_2q, and K_3r are the damping terms for roll, pitch, and heading, respectively.

The control surfaces were limited in travel to $+15^\circ$ and -45° for the rolling tail and to $\pm 6^\circ$ for the rudder. There were no rate limits nor limits on the autopilot authority. The physical properties of the control stick are given in table II.

A burnout warning lamp was included in the pilot's display. This lamp was provided to give the pilot a warning so that the trim changes that occur at burnout could be anticipated. This lamp came on 3 seconds before burnout and went out at engine thrust cutoff.

ANALOG PROGRAMING AND CHECKING

A complete schematic diagram of the analog simulation is shown in figure 12. Potentiometer settings for the diagram are given in table IV. The total amount of equipment used is as follows:

Amplifiers (total)	102
Integrators	15
Summers	37
Inverters	50
Potentiometers	109
Multipliers (shafts)	12
Potentiometers	33
Dual resolvers	2
Relay amplifiers	4

In order to check the analog setup, static and dynamic checks were made. Several digital check cases were run also. None of the check cases had any control inputs other than artificial damping.

For the program set up on the simulator, the dynamics of the problem were found to be near the critical region for the computer. Since the computer was to operate in conjunction with a pilot, a real time scale had to be accepted. In order to determine the effect of the dynamic error introduced by the analog computing elements, especially the servomultipliers, a digital check case without piloted controls was calculated. Runs made with different time scales on the analog setup showed that running the analog slow by 5:1 and 2.5:1 consistently gave the same results. Runs at a 1:1 time scale gave different results, without much

[redacted]

consistency. By meticulous choice of variables to drive the servo-multipliers, the 1:1 time-scale runs were made to check consistently those made at slower time scales. In this particular setup to obtain the products $m_z r$, $m_z p$, $n_z p$, and pr, the variables driving the servo-multiplier were changed: $m_z r$ from the m_z servo to the r servo, $m_z p$ from the m_z to the p servo, $n_z p$ from the n_z to the p servo, and pr from the p to the r servo. A comparison of the digital and analog results for one typical check case is shown in figure 13. In this case the only disturbance is the engine thrust misalinement.

An inspection of figure 13 shows some difference between the final analog setup and the digital calculation. In order to find if this magnitude of error is within the sensitivity of the analog equipment, two check cases were made. For one case the initial angles of attack and sideslip were equal to 0.1 radian, and for the other case both angles were 0.105 radian. It was found that this 5-percent difference in input would more than account for the differences in the digital and analog results of figure 13 and that final results similar to those of figure 13 could be considered reasonable. It was felt, however, that with the availability of more servomultipliers or if electronic multipliers had been available, the dynamic error could have been reduced.

Another trouble spot was the calculation of the direction cosines. Here it was found that the static nulling error of the servomultipliers was important because of the output voltage possible for zero input to the servomultiplier when a large voltage was impressed across the multiplying potentiometer. This was found to be particularly critical in the $n_z p$ product in equation (7). Because of the dynamics involved, this product was calculated on the p-multiplier but better static accuracy would result if the product was obtained from a servomultiplier driven by n_z. Thus, it was necessary that this multiplying potentiometer be set carefully on zero. The use of diode-type multipliers may be warranted because of their good zero output for zero-input characteristics and their good frequency response.

The static stability derivatives which were functions of Mach number could be expressed as functions of flight time (see table III and fig. 4) because of the programing of Mach numbers. Terms such as $C_{l_\beta}\beta$ and $C_{L_\alpha}\alpha$ were then written as the product of a polynomial in t and α or β. As shown in figure 12, this permits the static stability derivatives to be generated on servomultipliers driven by $\dot{t}$ and t^2 which are slowly changing variables compared with α and β.

STARTING THE ANALOG

In the check case shown in figure 13 the motions start abruptly because of the engine thrust misalinement in pitch attitude and heading. In the piloted runs which had thrust misalinement, the pilot was allowed to fly at a constant Mach number until the misalinement could be trimmed out. The flight-plan trajectory was then started. This procedure allowed a smooth controlled start on the trajectory with the only abrupt change in trim occurring at burnout.

[redacted]

TABLE I

CONTROL-SURFACE-EFFECTIVENESS COEFFICIENTS

[$M = 3.5$; $\alpha = \beta = 0$]

$C_{l_{\delta_h}}$, per radian	-0.0344
$C_{n_{\delta_h}}$, per radian	-0.0144 (varied from 0.0504 to -0.0144)
$C_{y_{\delta_h}}$, per radian	-0.0172
$C_{y_{\delta_v}}$, per radian	-0.2037
$C_{n_{\delta_v}}$, per radian	-0.143
$C_{l_{\delta_v}}$, per radian	0.0527 (or -0.0527)
$C_{m_{\delta_h}}$, per radian	-0.344

[redacted]

TABLE II

CONTROL-SURFACE MOVEMENTS AND FORCES

Control	Stick or pedal movement, in.	Force, lb	Surface deflection, deg
Horizontal	2.5	10	45
Horizontal-tail roll control	4	10	24 (total)
Vertical tail	1	50	6

TABLE III

PROGRAMED DATA

	$0 \leqq t < 28$ sec	$28 \leqq t \leqq 50$ sec
V, ft/sec	$3150 + 104t$	6062
M	$3.2 + 0.082t$	5.496
q_d, lb/sq ft	$350 - 12.4t + 0.116t^2$	$350 - 12.4t + 0.116t^2$
I_x, slug-ft^2	$5519 - 17.8t$	5021
I_y, slug-ft^2	$73425 - 298t$	65110
I_z, slug-ft^2	$75563 - 299t$	67200
m, slugs	$567.8 - 6.335t$	390.4
C_{l_β}, per radian	$-0.04469 + 0.0004699t$	-0.03153
C_{m_o}	$-0.009643t + 0.00003285t^2$	-0.001246
C_{m_α}, per radian	$-0.6148 + 0.01908t - 0.0001426t^2$	-0.1924
C_{n_β}, per radian	$0.1015 - 0.007847t + 0.0000865t^2$	-0.0504
C_{L_α}, per radian	$2.12 - 0.02678t$	1.370
C_{y_β}, per radian	$-0.7697 + 0.0137t - 0.0001609t^2$	-0.5122

TABLE IV.- POTENTIOMETER SETTINGS AND GAINS

Potentiometer	Setting	Gain
1	0.013	1
2	0	1
3	.659	1
4	.560	1
5	.235	1
6	.537	4
7	.537	4
8	.280	1
9	$-.125C_{l_r}$	1
10	$-.125C_{l_p}$	10
11	.694	1
12	.800	1
13	.358	4
14	.349	Recorder
15	$10^{-5}E_{M_v}$	1
16	.438	4
17	.261	1
18	.307	1
19	.382	1
20	.071	1
21	.096	1
22	.082	1
23	0	1
24	.430	1
25	.430	1
26	.257	1
27	---	---
28	$-.0025C_{m_q}$	1
29	$-.005C_{m_{\dot{\alpha}}}$	1
30	.411	10
31	.424	4
32	.280	1
33	$10^{-5}E_{M_E}$	1
34	.508	1
35	.392	4
36	.432	1
37	.716	1
38	.286	1
39	.286	1
40	.140	4
41	$-.025C_{L_r}$	1
42	$.25C_{n_p}$	1
43	.894	1
44	1.000	1
45	.500	1
46	.080	1
47	.818	1
48	.428	1
49	.100	1

Potentiometer	Setting	Gain
50	.042	1
51	.050	1
52	.500	1
53	.080	1
54	.042	1
55	.308	1
56	.219	1
57	.064	1
58	.121	1
59	.100	1
60	.050	1
61	.500	10
62	.418	I.C.
63	.500	1
64	.500	1
65	.500	10
66	.500	1
67	.682	I.C.
68	.500	1
69	.500	10
70	$-.5K_1$	10
71	$.5K_2$	1
72	Bias	1
73	.880	Recorder
74	.702	1
75	.702	1
76	.873	4
77	Bias	1
78	$-.5K_1$	10
79	$.5K_2$	1
80	.616	Recorder
81	Bias	1
82	.674	4
83	$.625K_3$	4
84	.550	I.C.
85	.100	---
86	.250	1
87	.080	1
88	.416	1
89	.315	1
90	.119	1
91	.071	1
92	.552	1
93	.734	1
94	.756	1
95	.568	1
96	.120	1
97	.253	1
98	.992	1
99	.032	1
100	---	---
101	.580	1
102	.700	1
103	.700	1

[redacted]

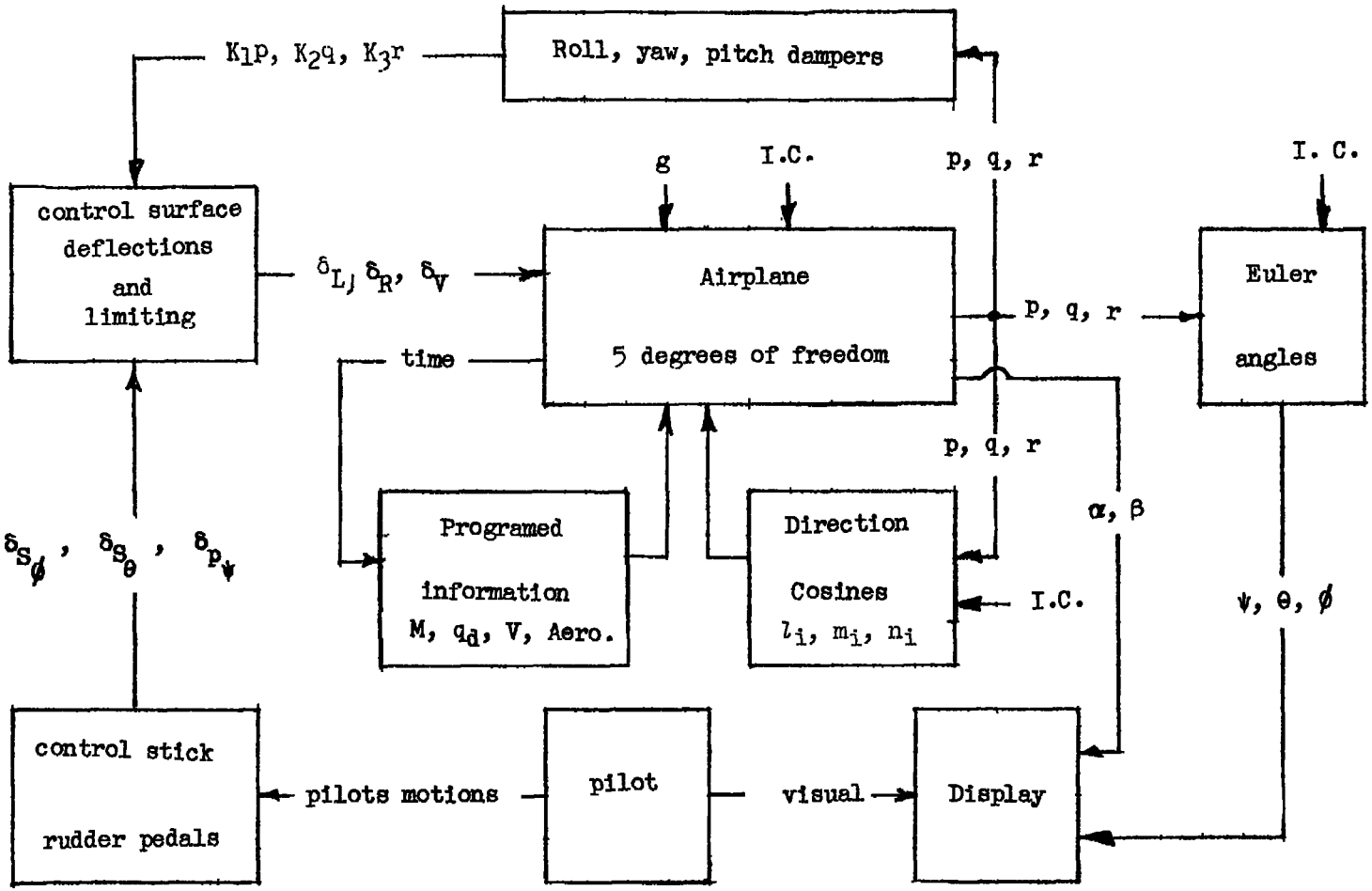

Figure 1.- Block diagram of the problem as set up for study on the analog computer.

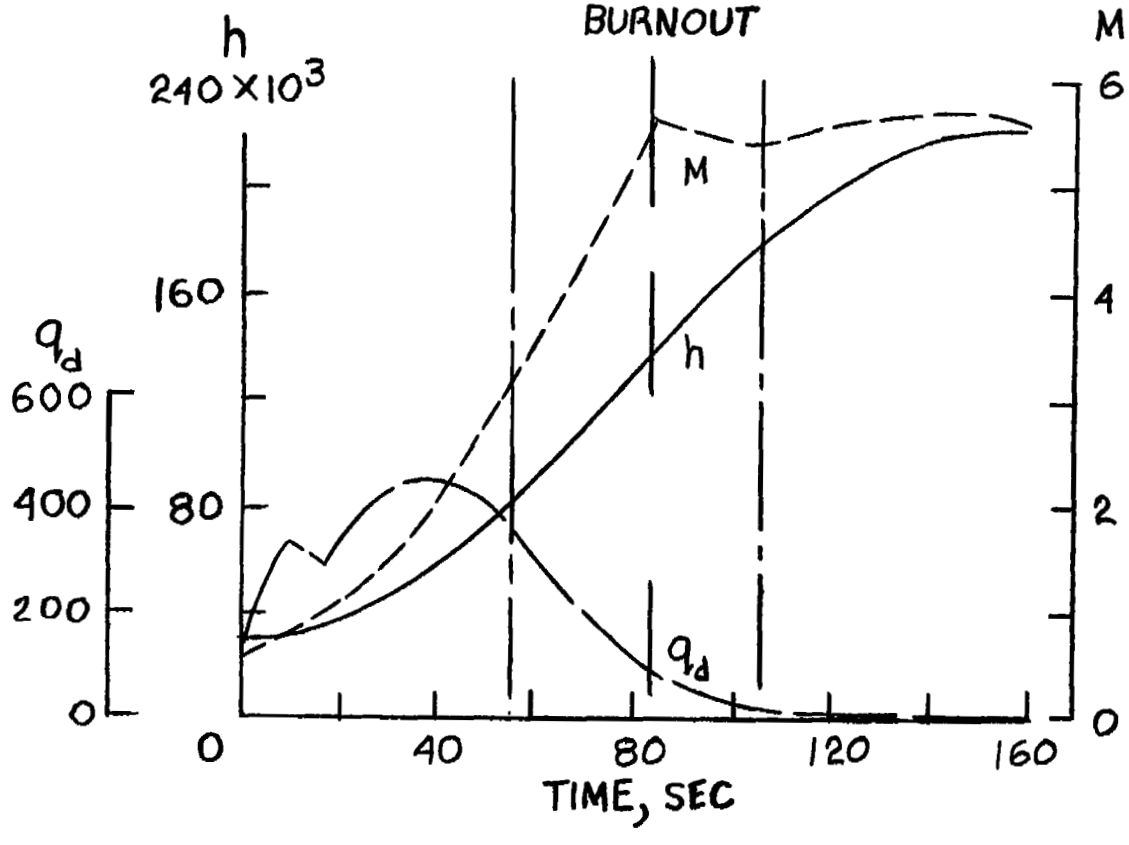

Figure 2.- Variations of the altitude, dynamic pressure, and Mach number with flight time assumed for this investigation.

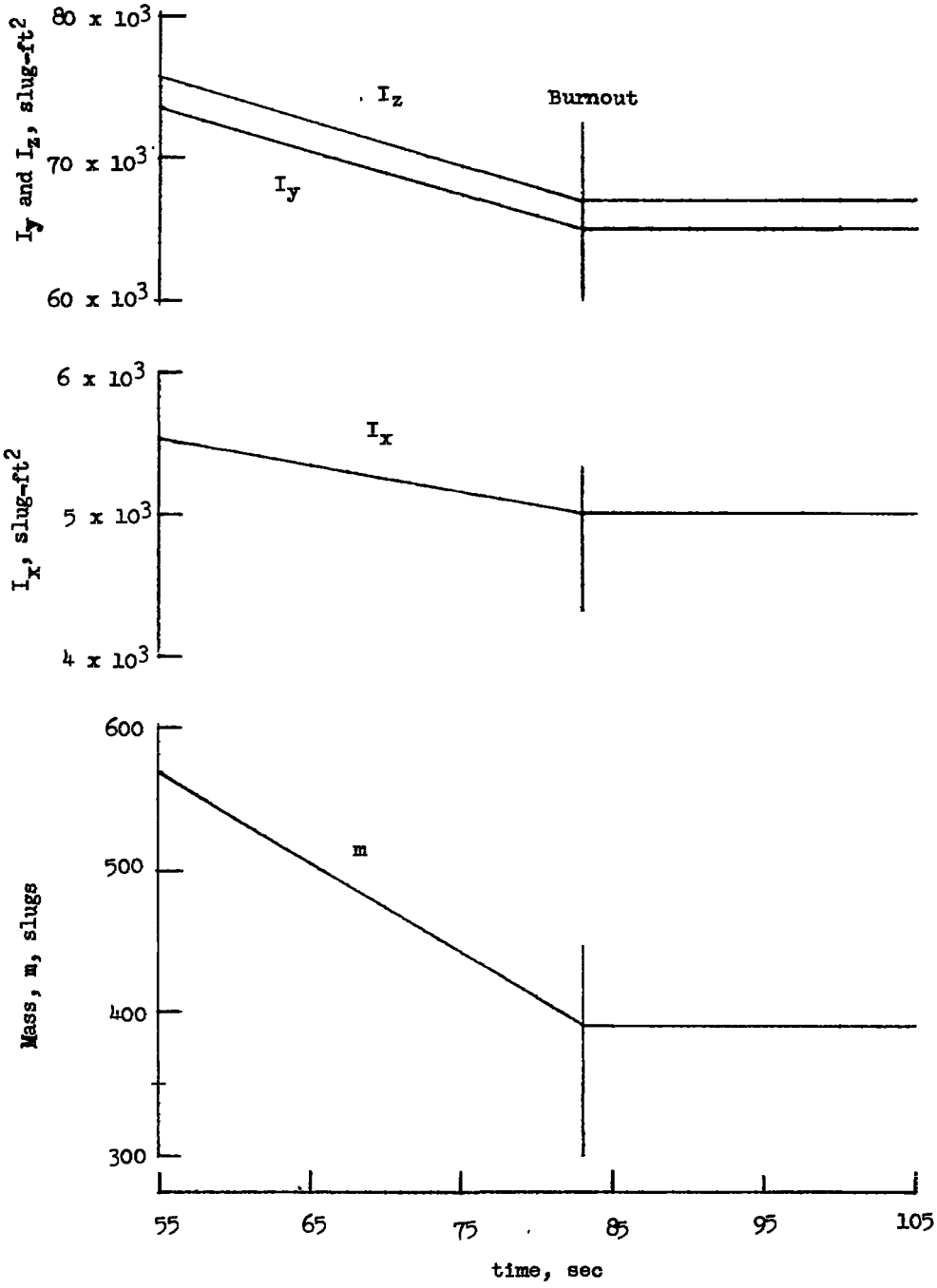

Figure 3.- Assumed variations of the moments of inertia and mass with time.

[redacted]

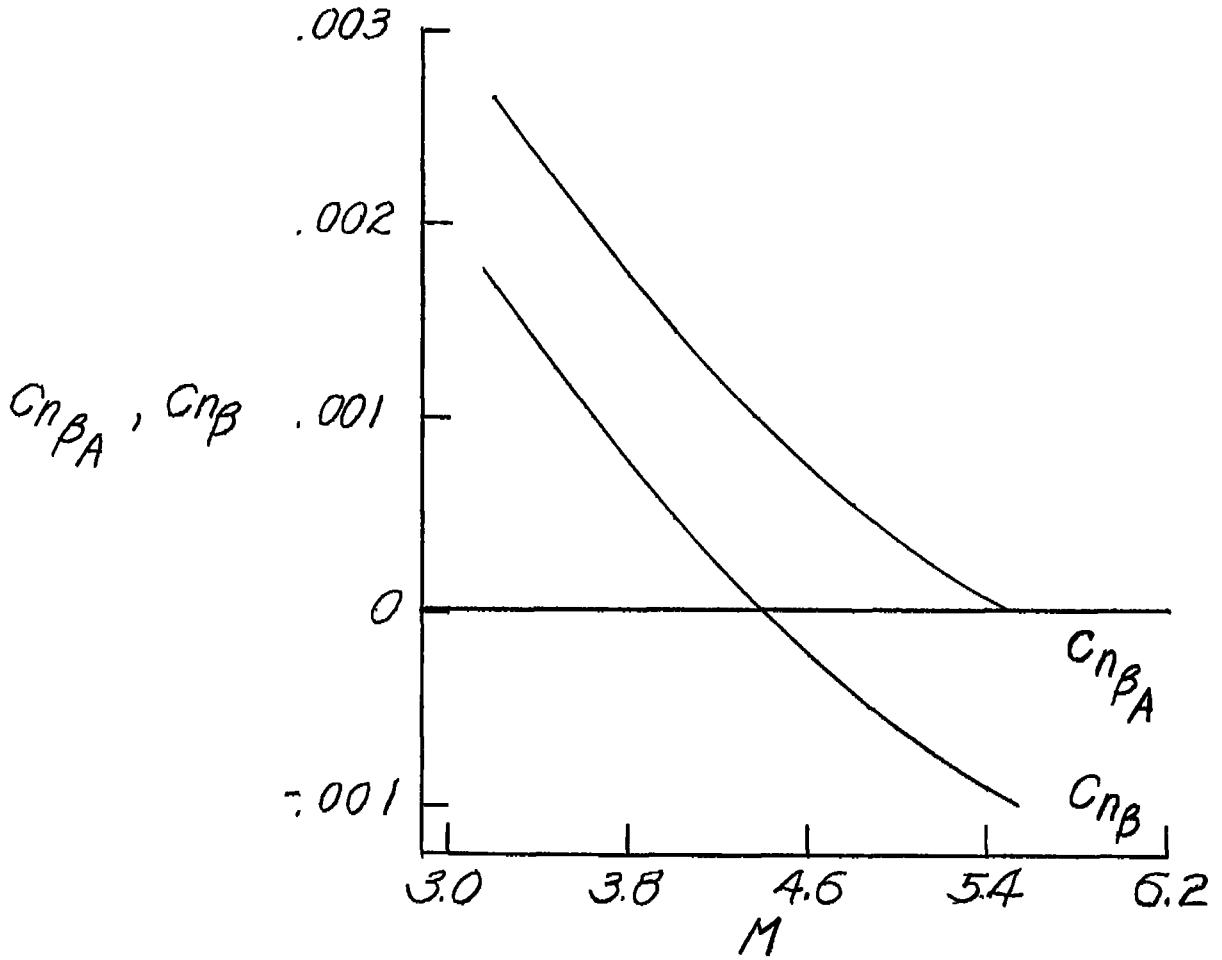

(a) C_{n_β}.

Figure 4.- Variation of the static stability derivatives with Mach number. All stability derivatives are presented per degree variation of α and β.

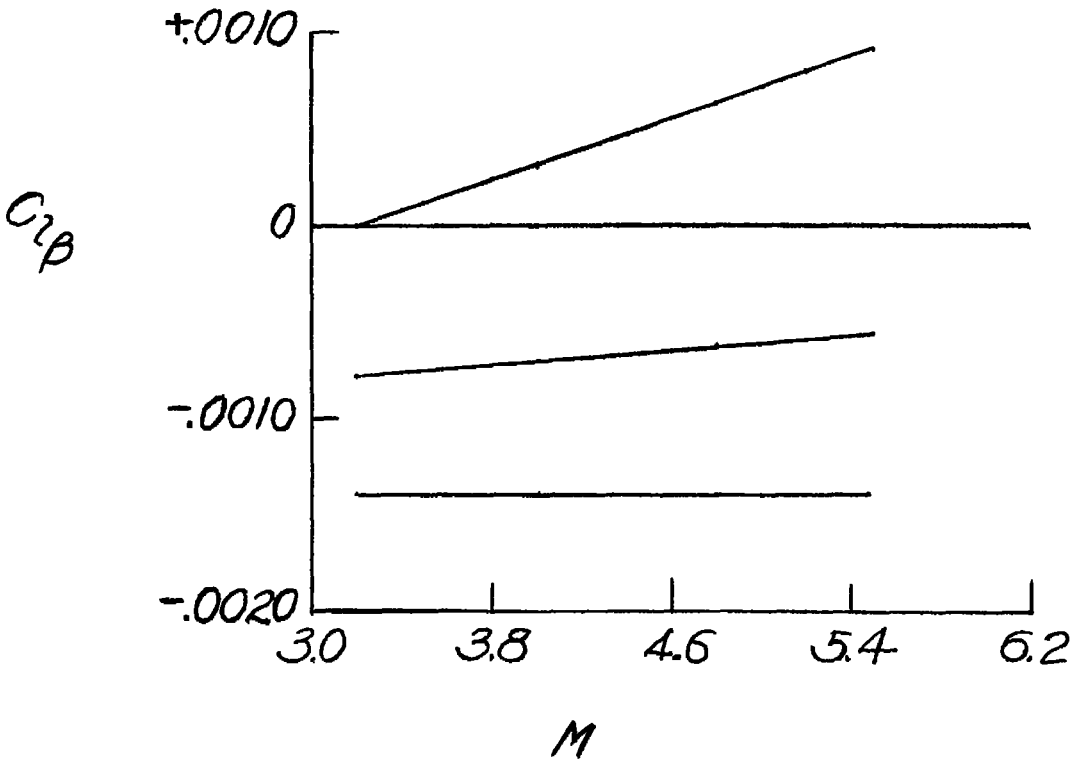

(b) C_{l_β}.

Figure 4.- Continued.

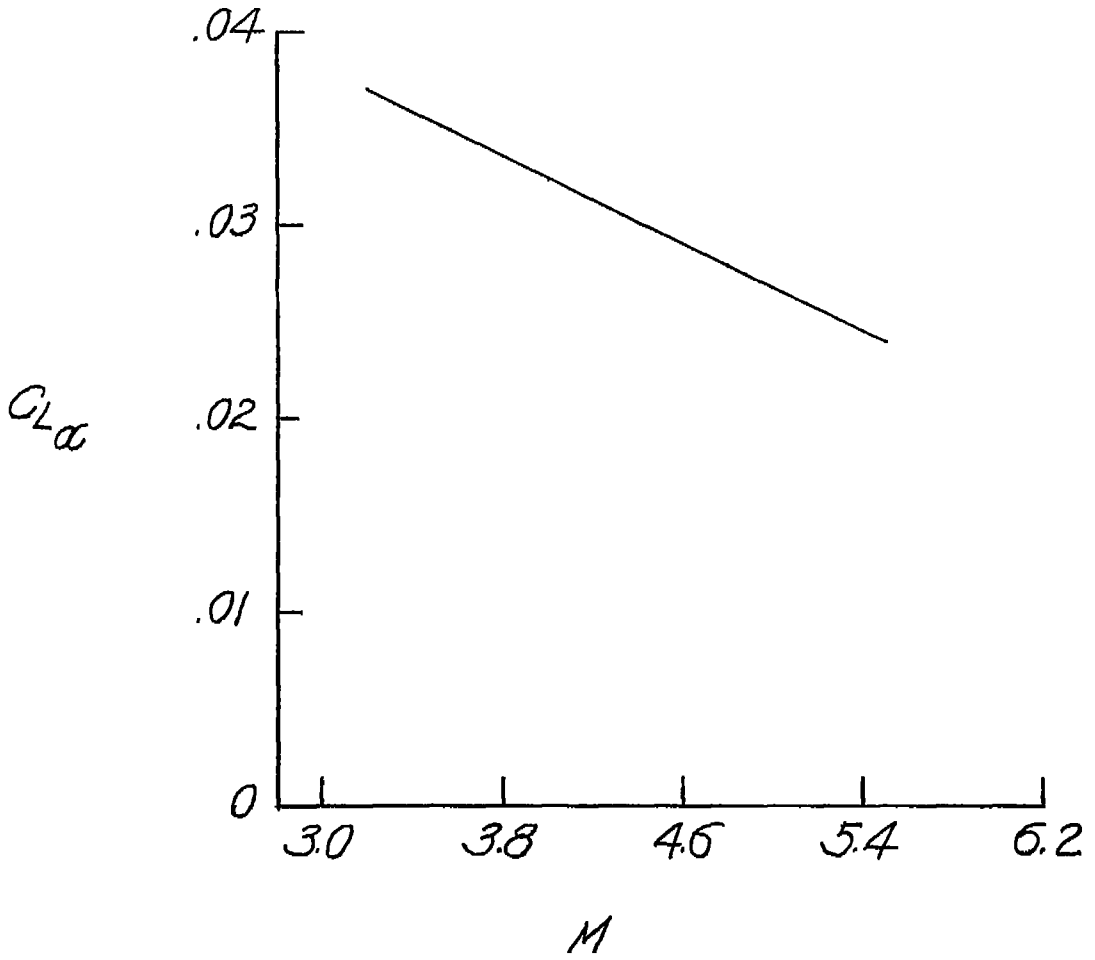

(c) C_{l_α}.

Figure 4.- Continued.

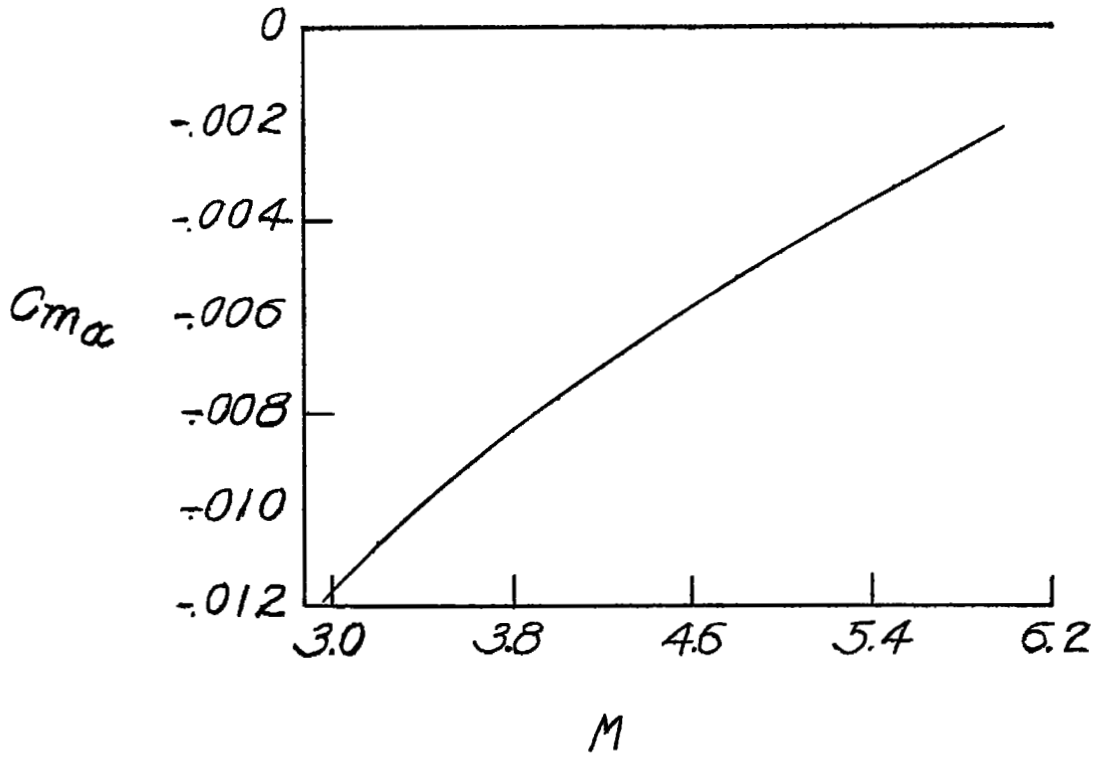

(d) C_{m_α}.

Figure 4.- Continued.

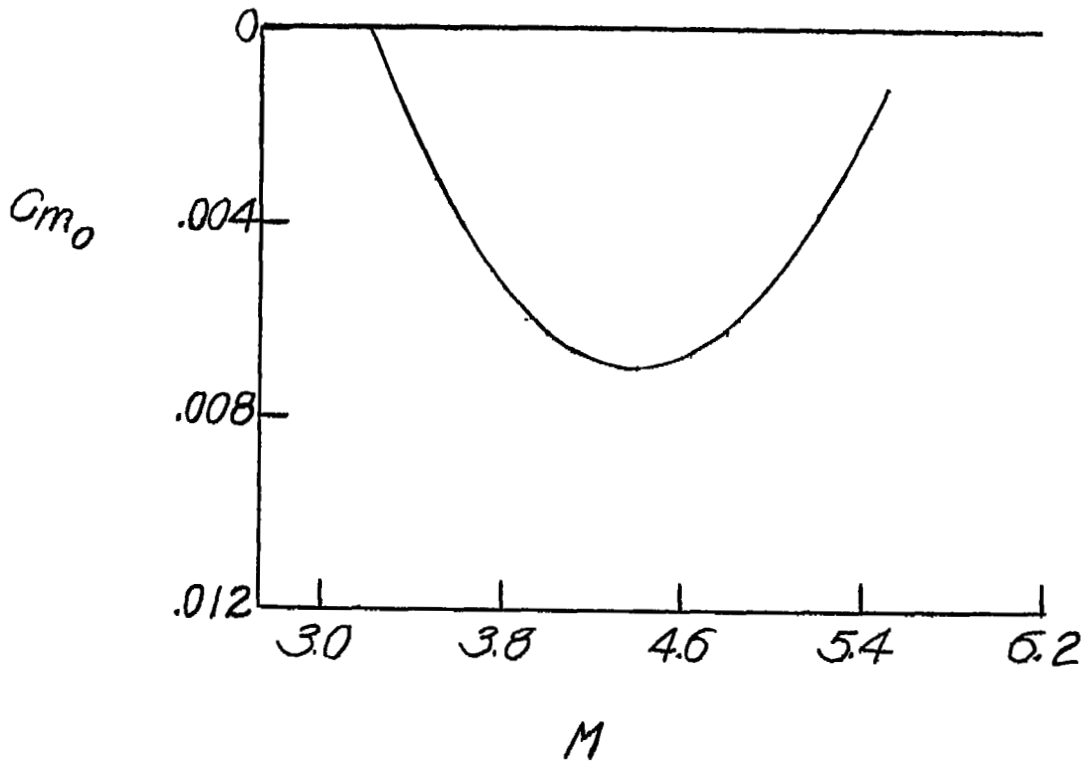

(e) C_{m_o}.

Figure 4.- Continued.

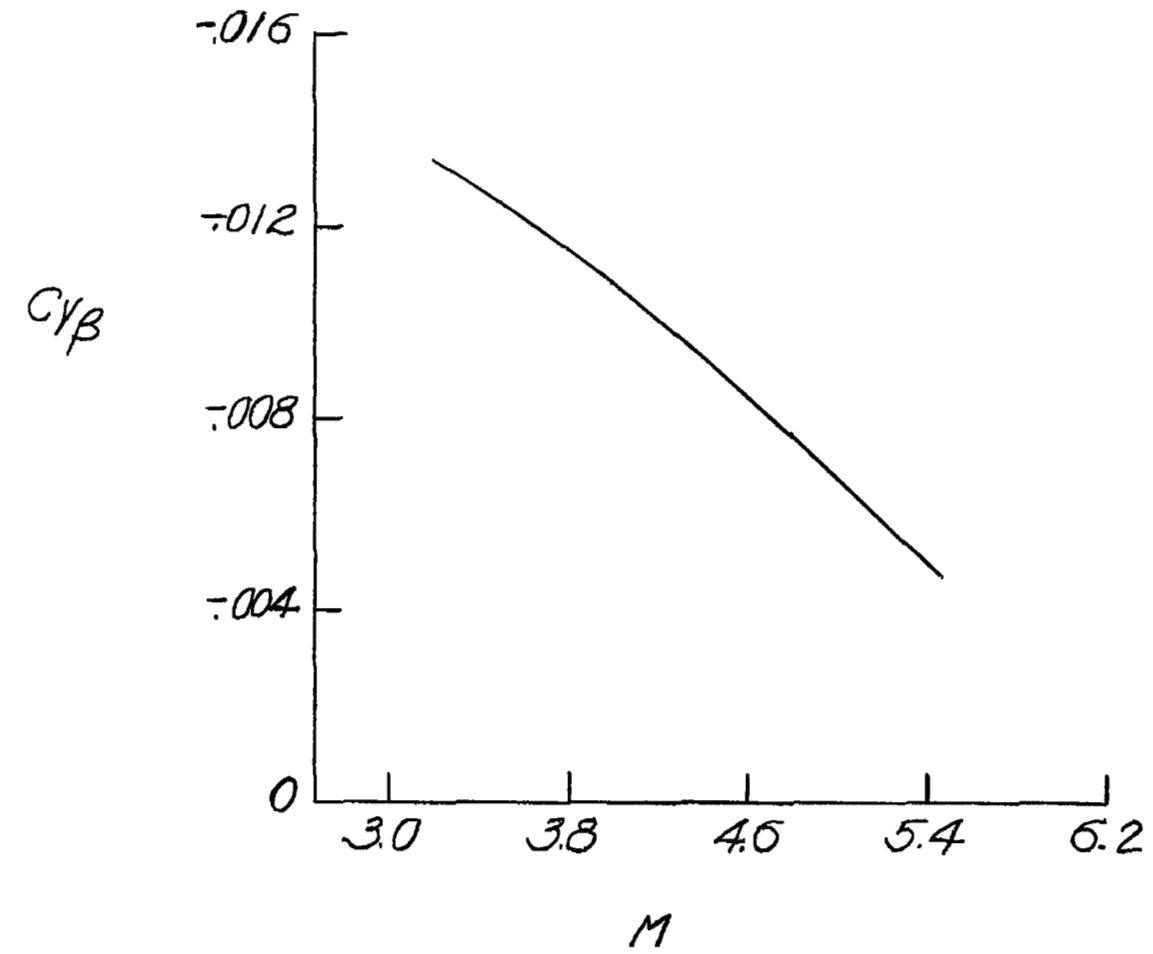

(f) C_{Y_β}.

Figure 4.- Concluded.

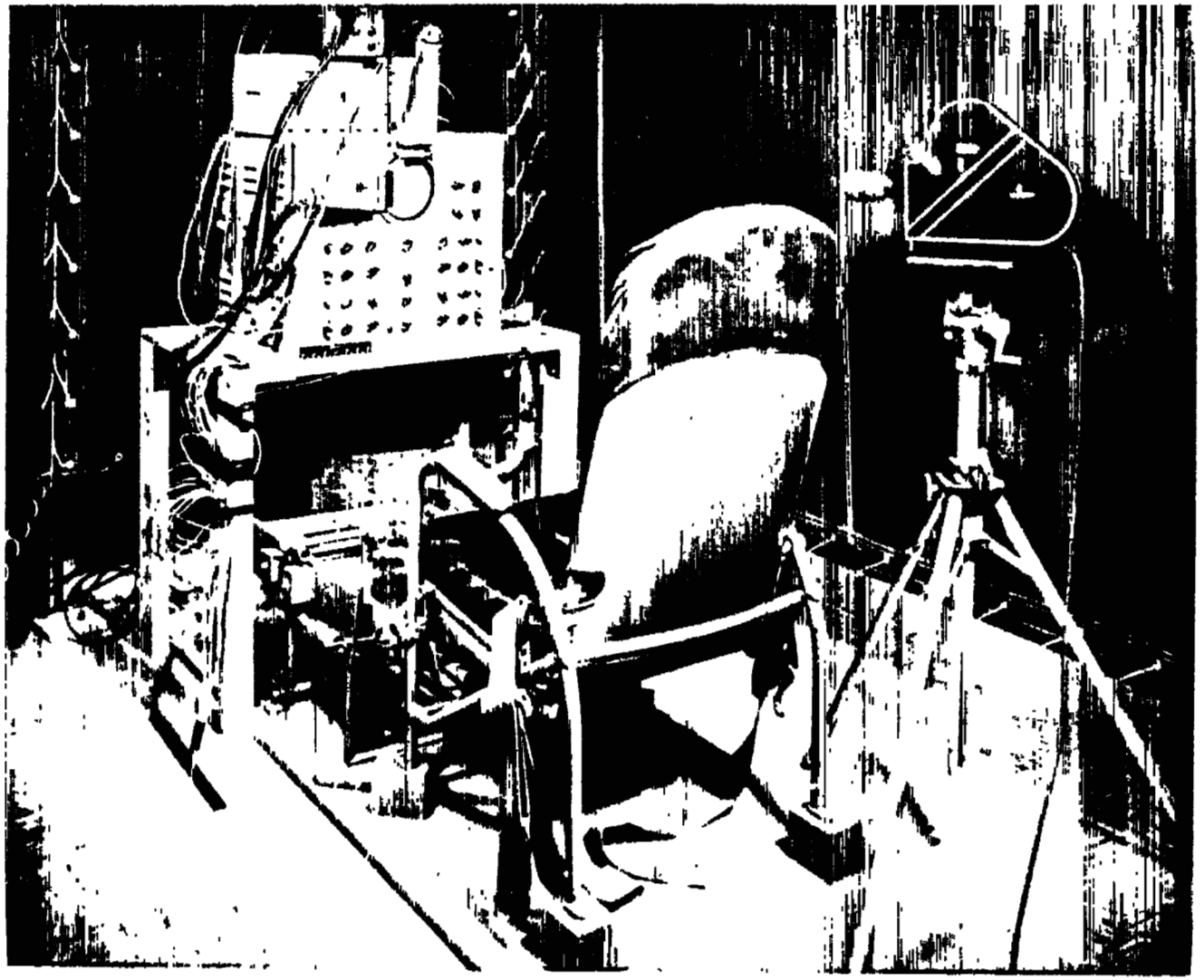

Figure 5.- Pilot's control station. L-95262

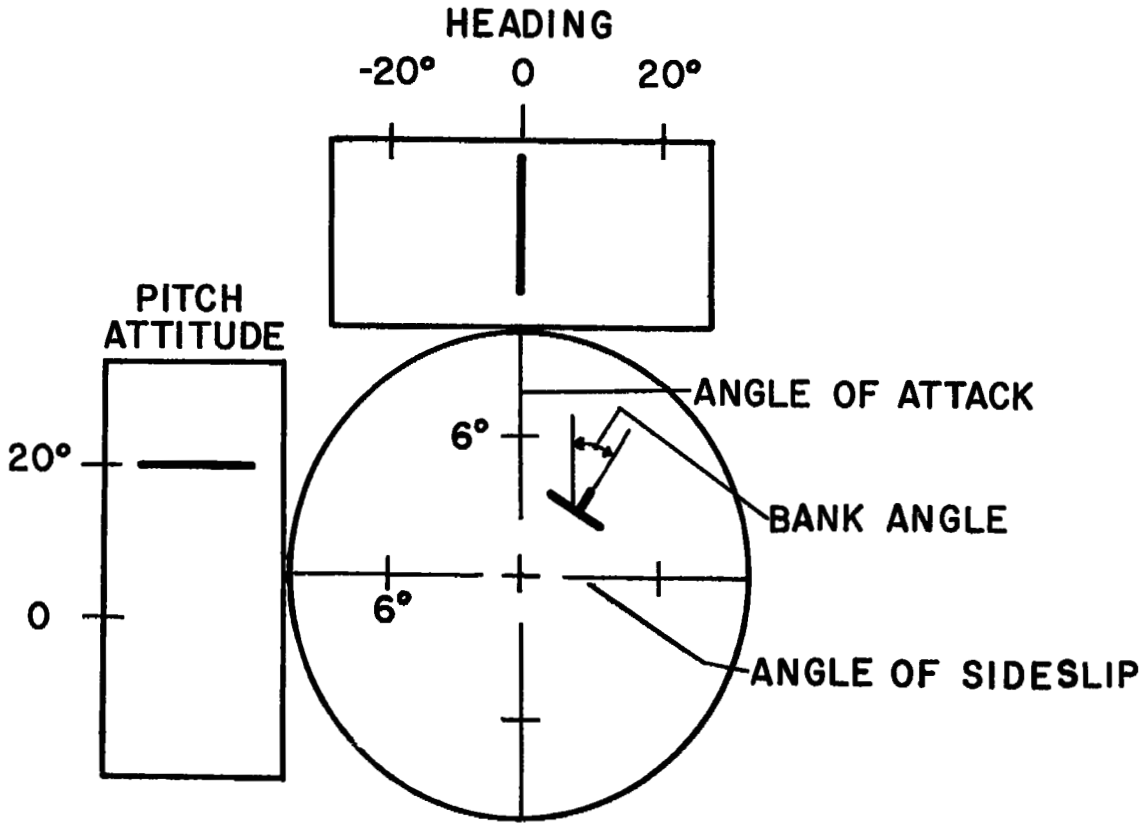

Figure 6.- Sketch showing details of information display.

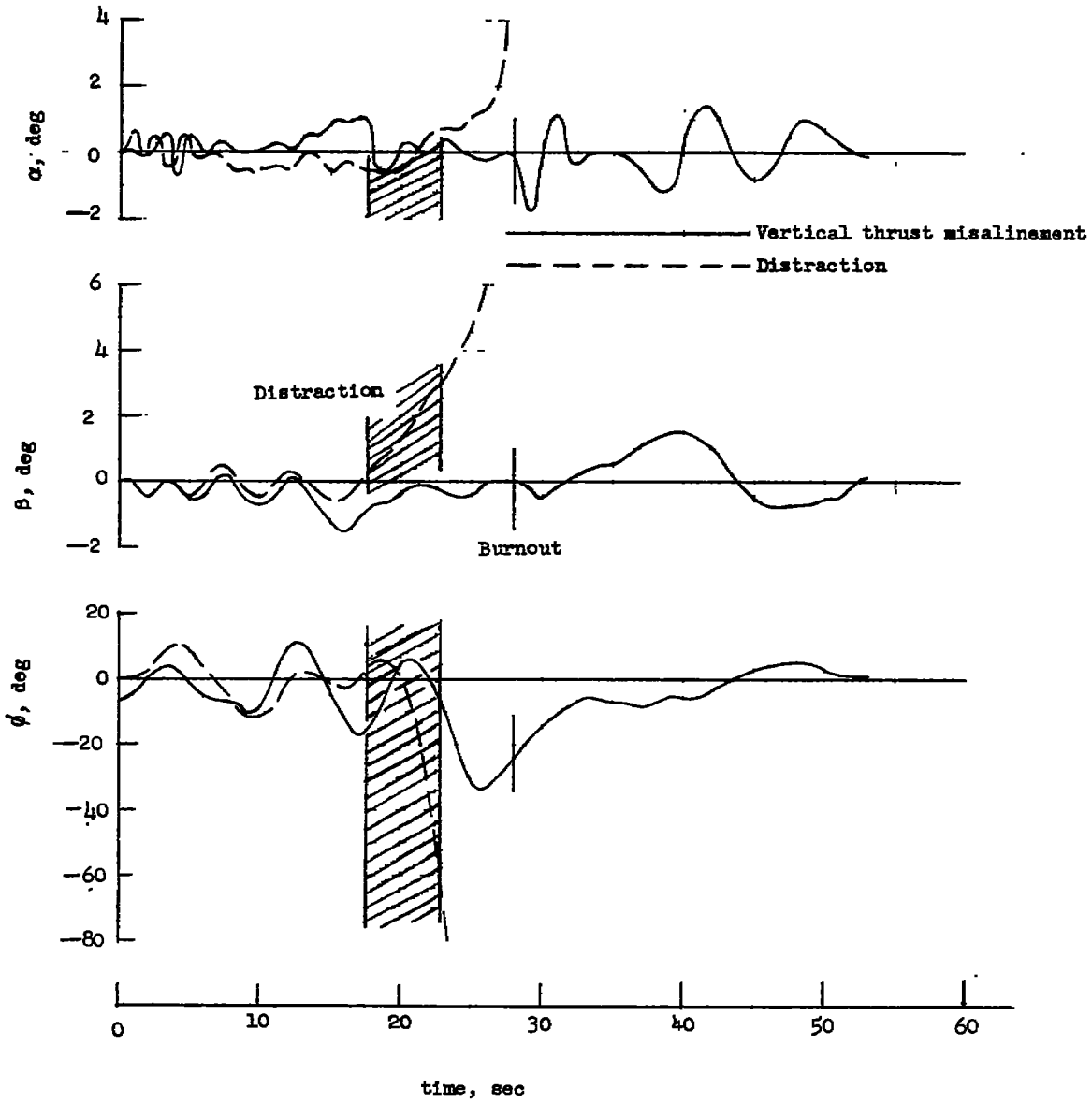

(a) Distraction and vertical thrust misalinement.

Figure 7.- The effect of pilot distraction and engine moments on the ability of the pilot to control the airplane.

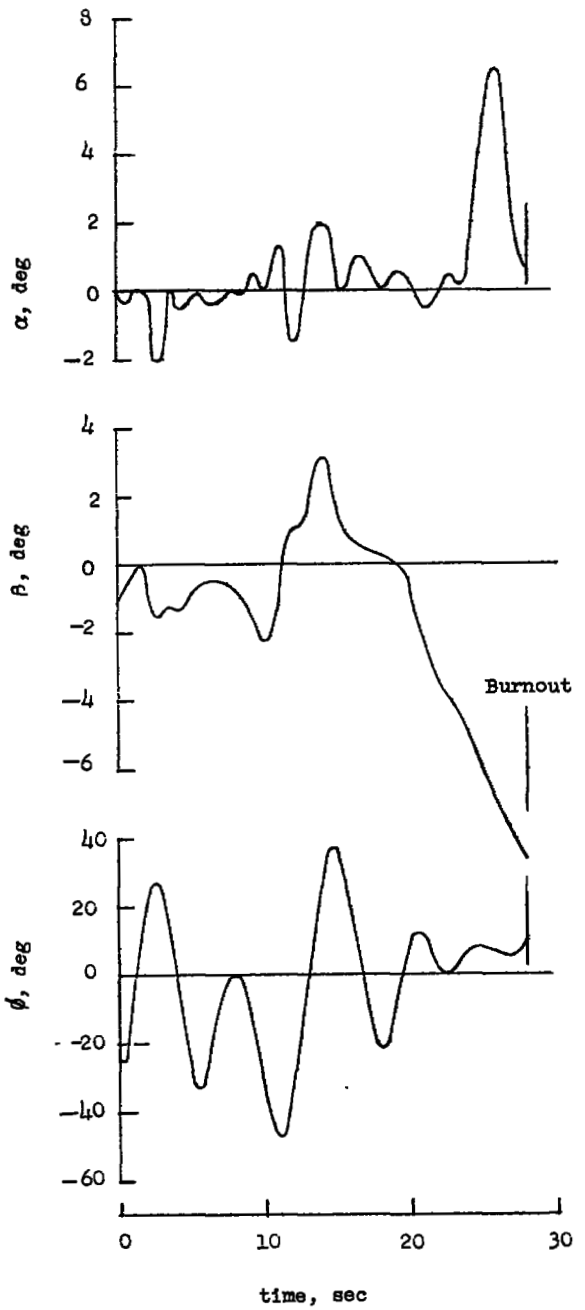

(b) Vertical and horizontal thrust misalinements.

Figure 7.- Concluded.

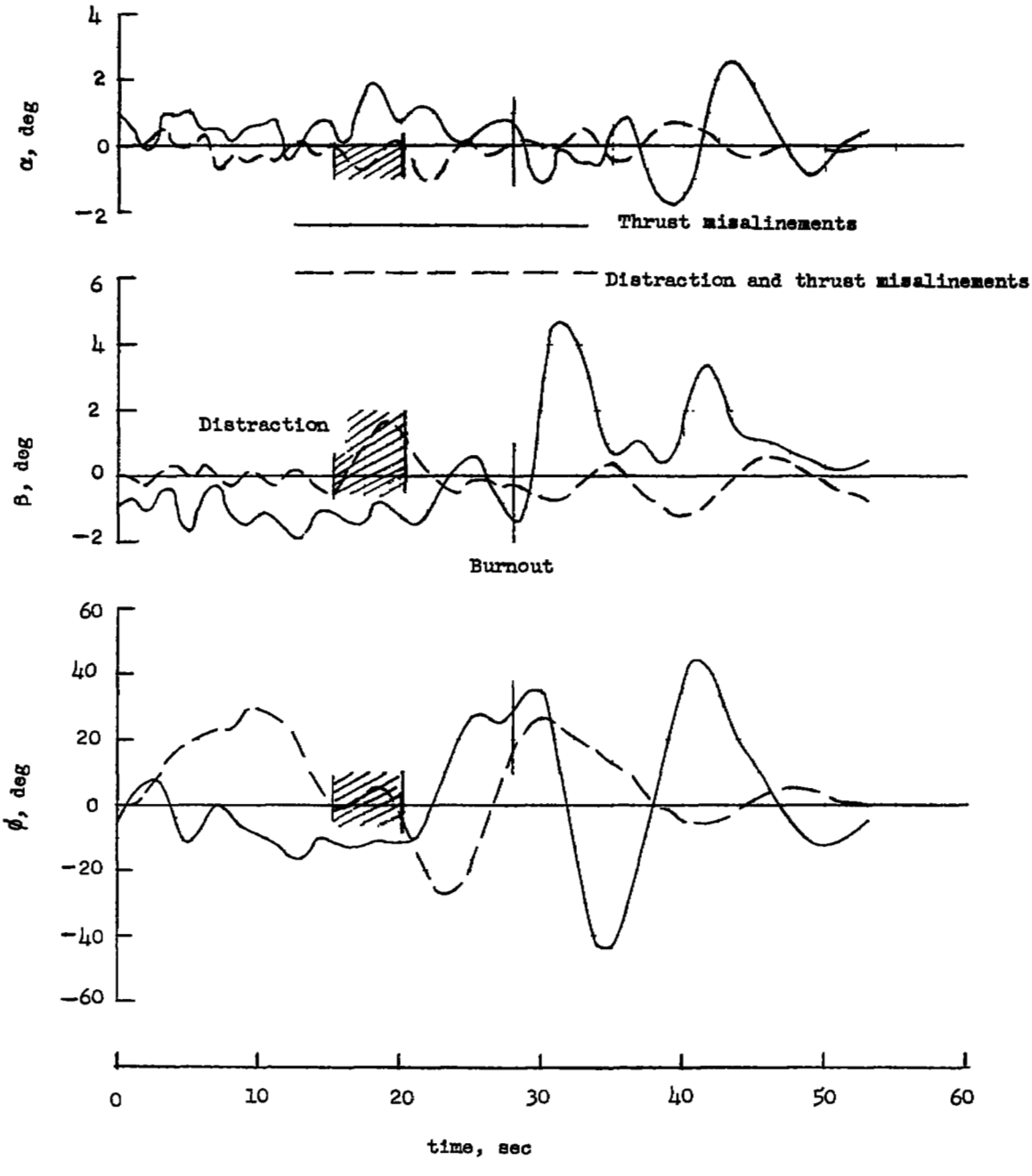

Figure 8.- Pilot control of simulated airplane with increased C_{n_β}, $C_{n_{\beta_A}}$ of figure 4(a).

[redacted]

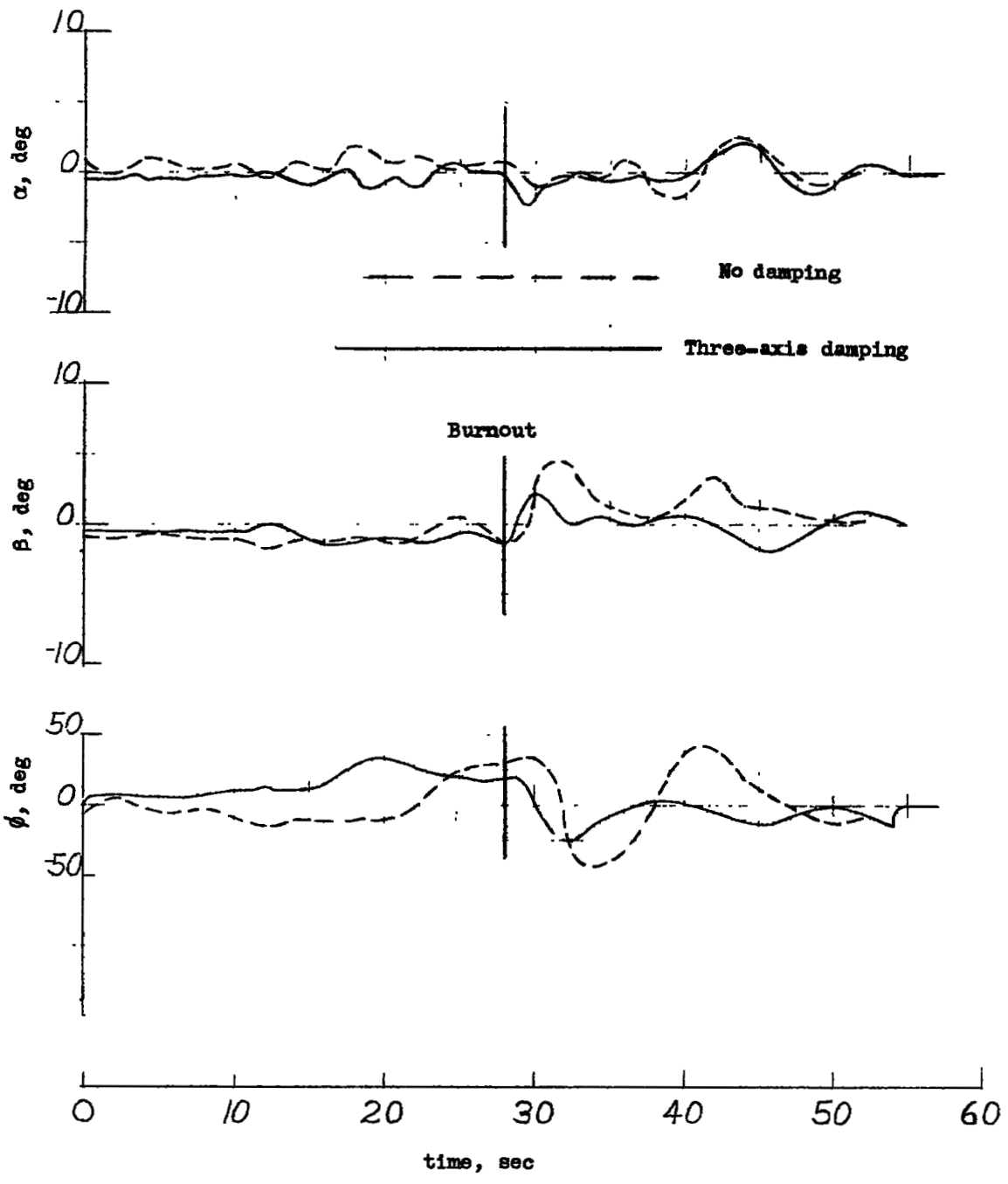

Figure 9.- The effect of three-axis damping on the ability of the pilot to control the airplane.

[redacted]

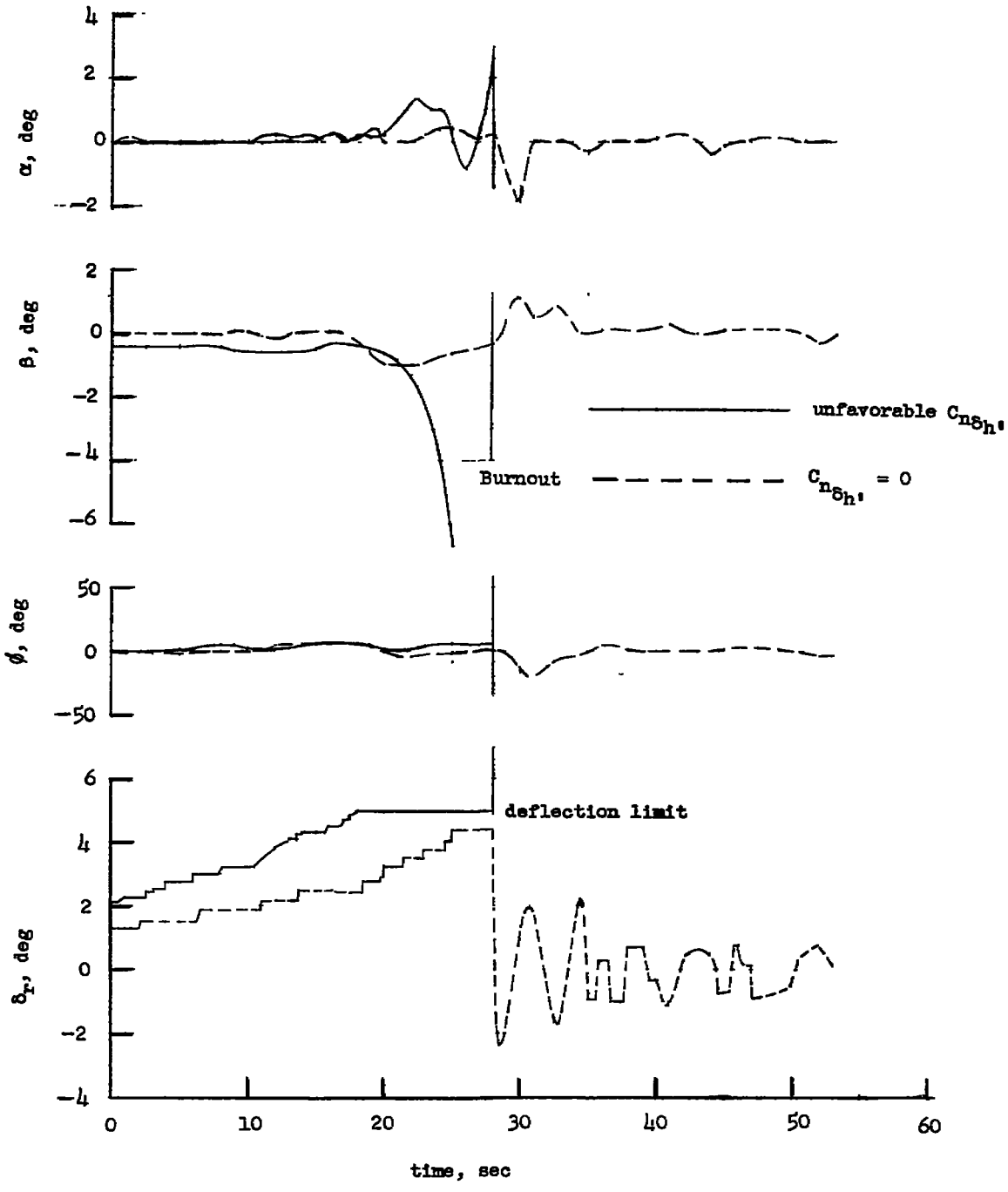

Figure 10.- The effect of $C_{n_{\delta_{h'}}}$ on the controllability of the airplane.

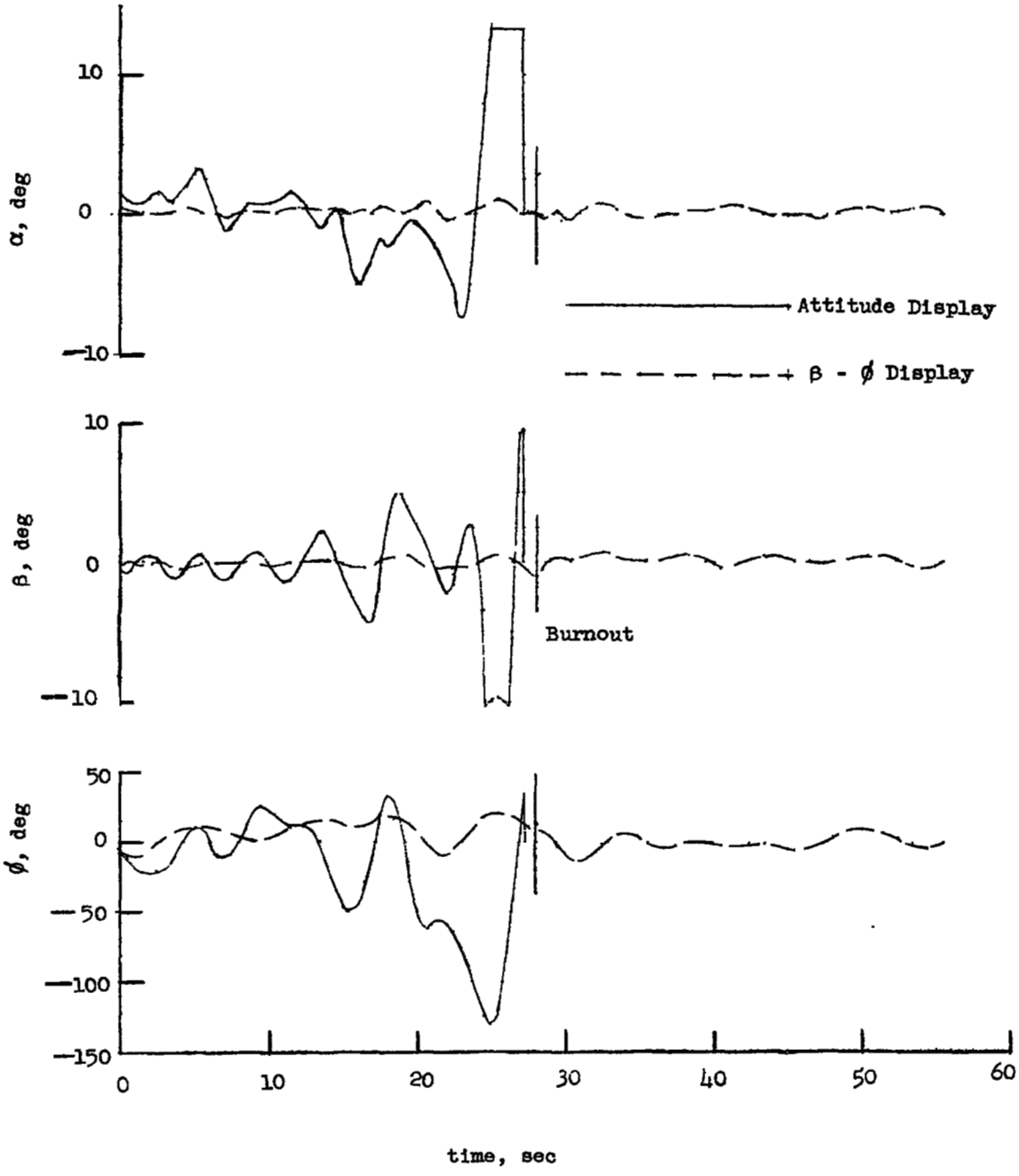

Figure 11.- The effect of changing the display on the control task.

[redacted]

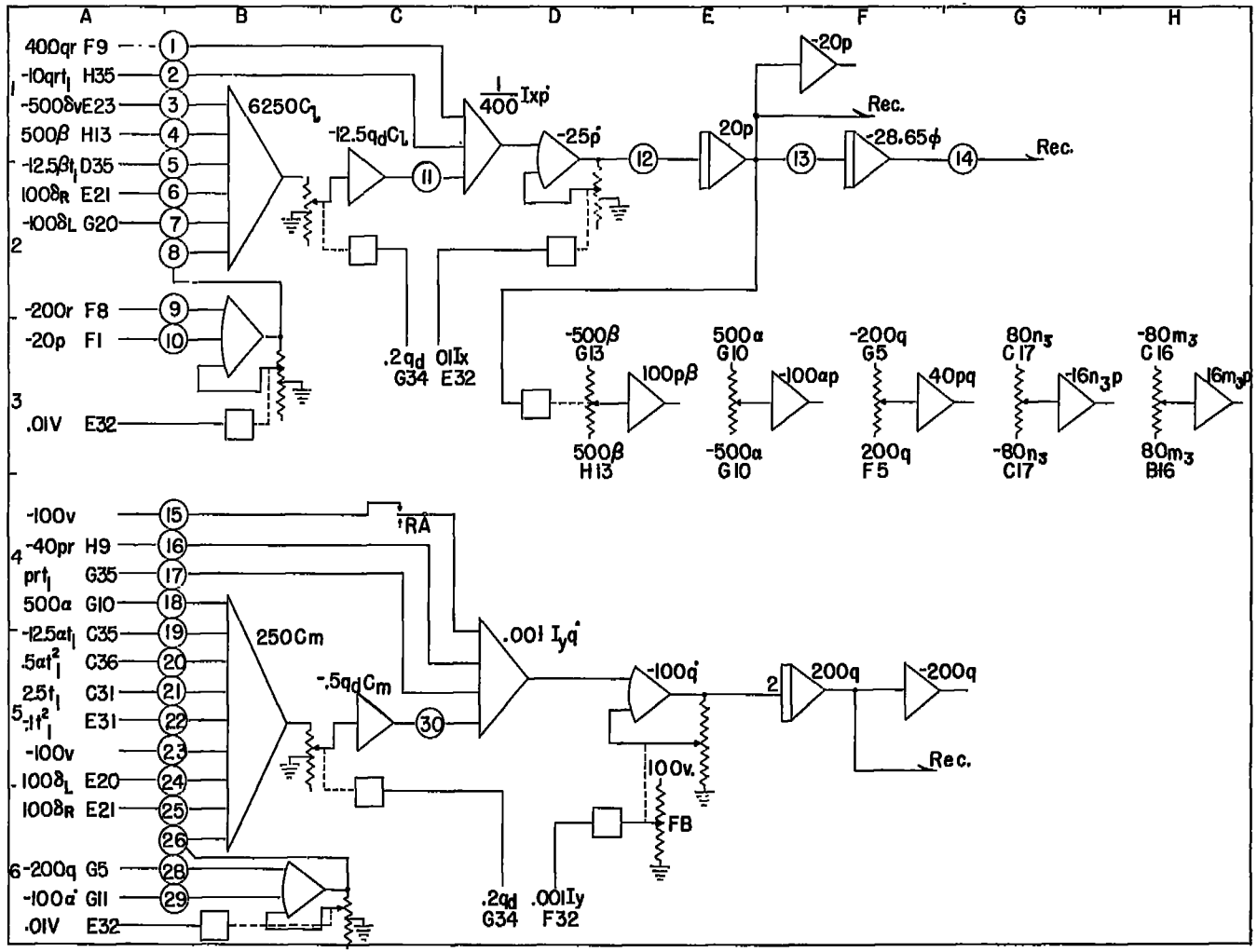

(a) Rolling and pitching circuit.

Figure 12.- Schematic diagram of analog simulation.

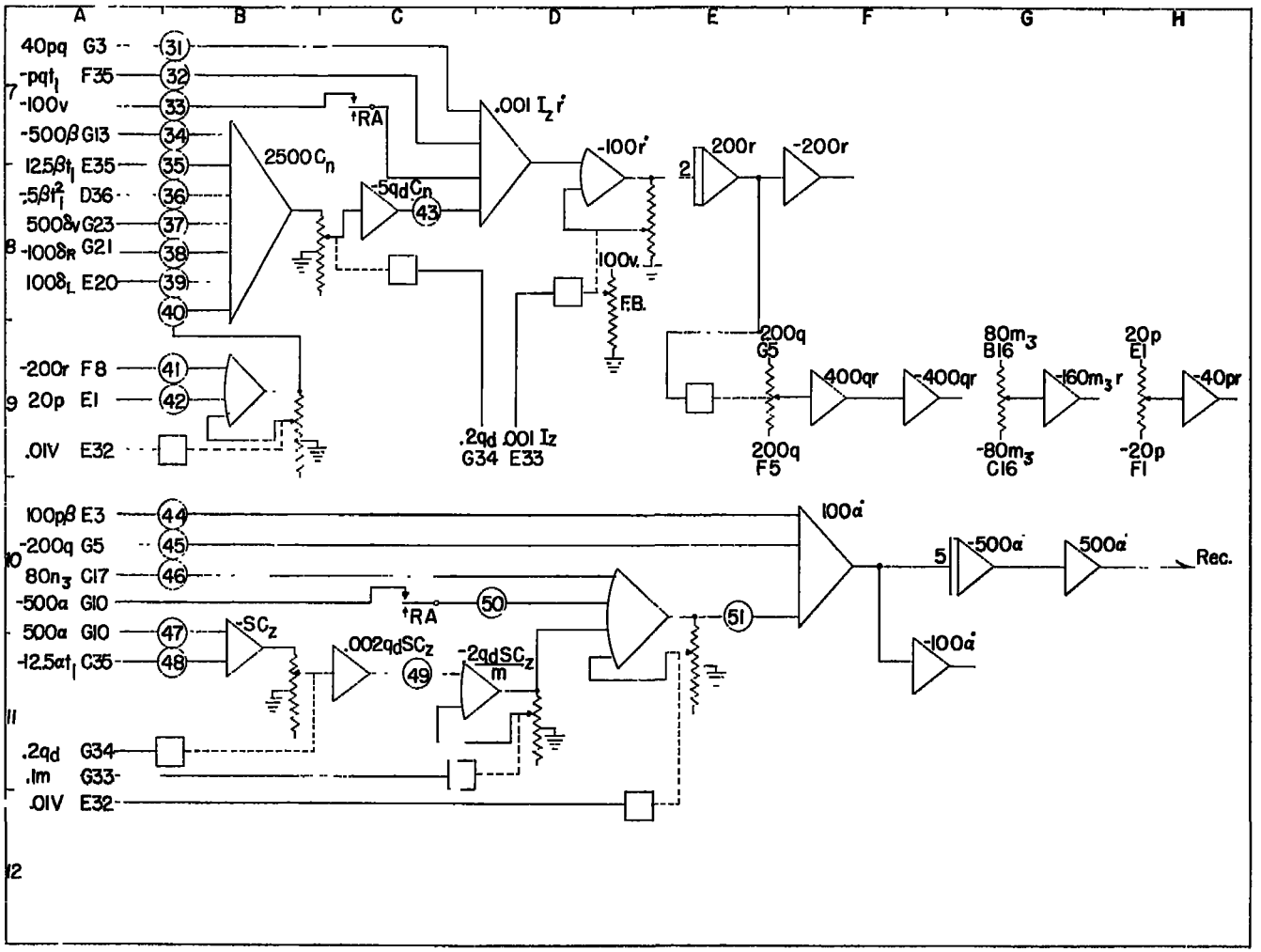

(b) Yawing and angle-of-attack circuit.

Figure 12.- Continued.

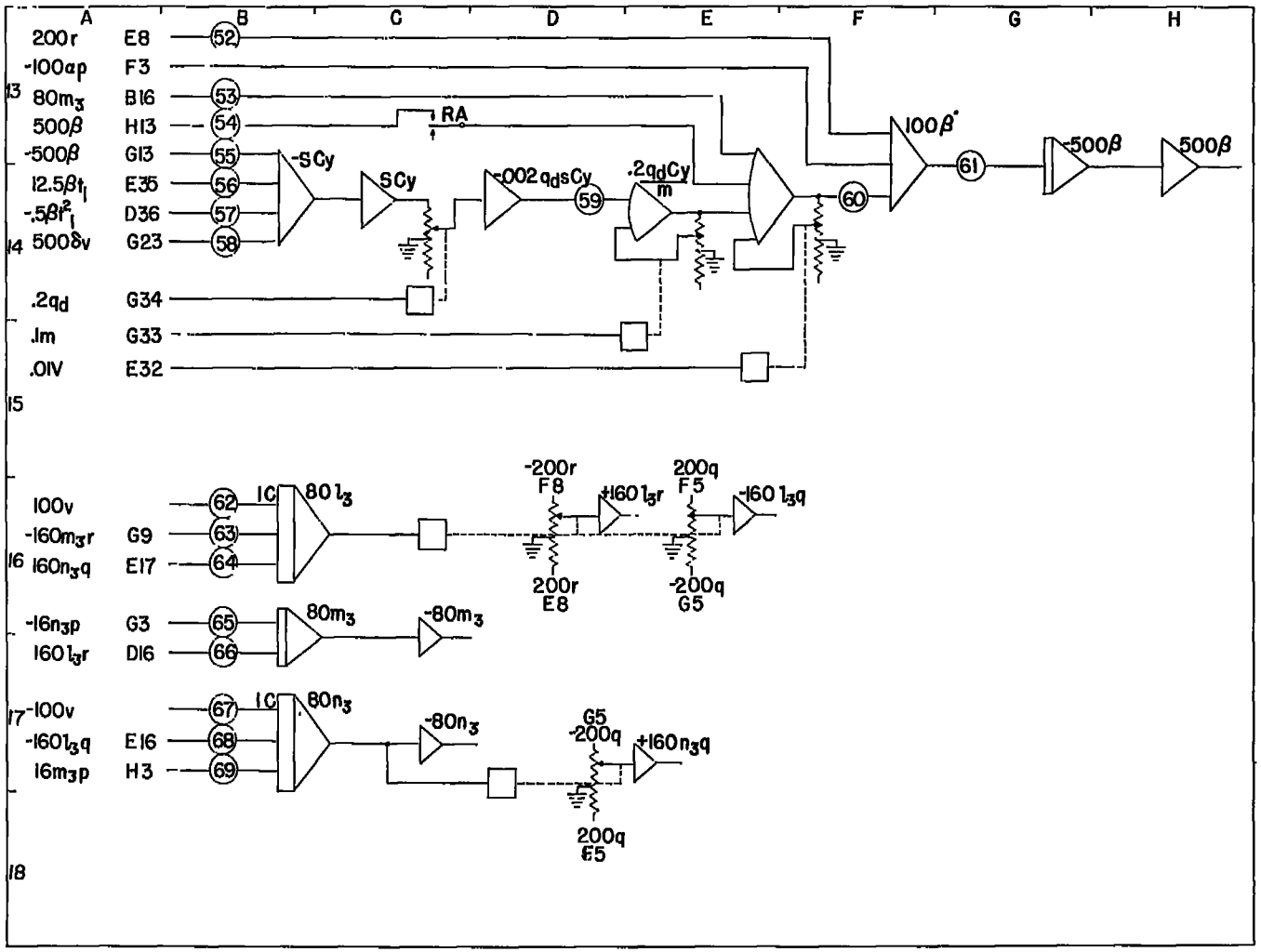

(c) Angle-of-sideslip and direction cosine circuit.

Figure 12.- Continued.

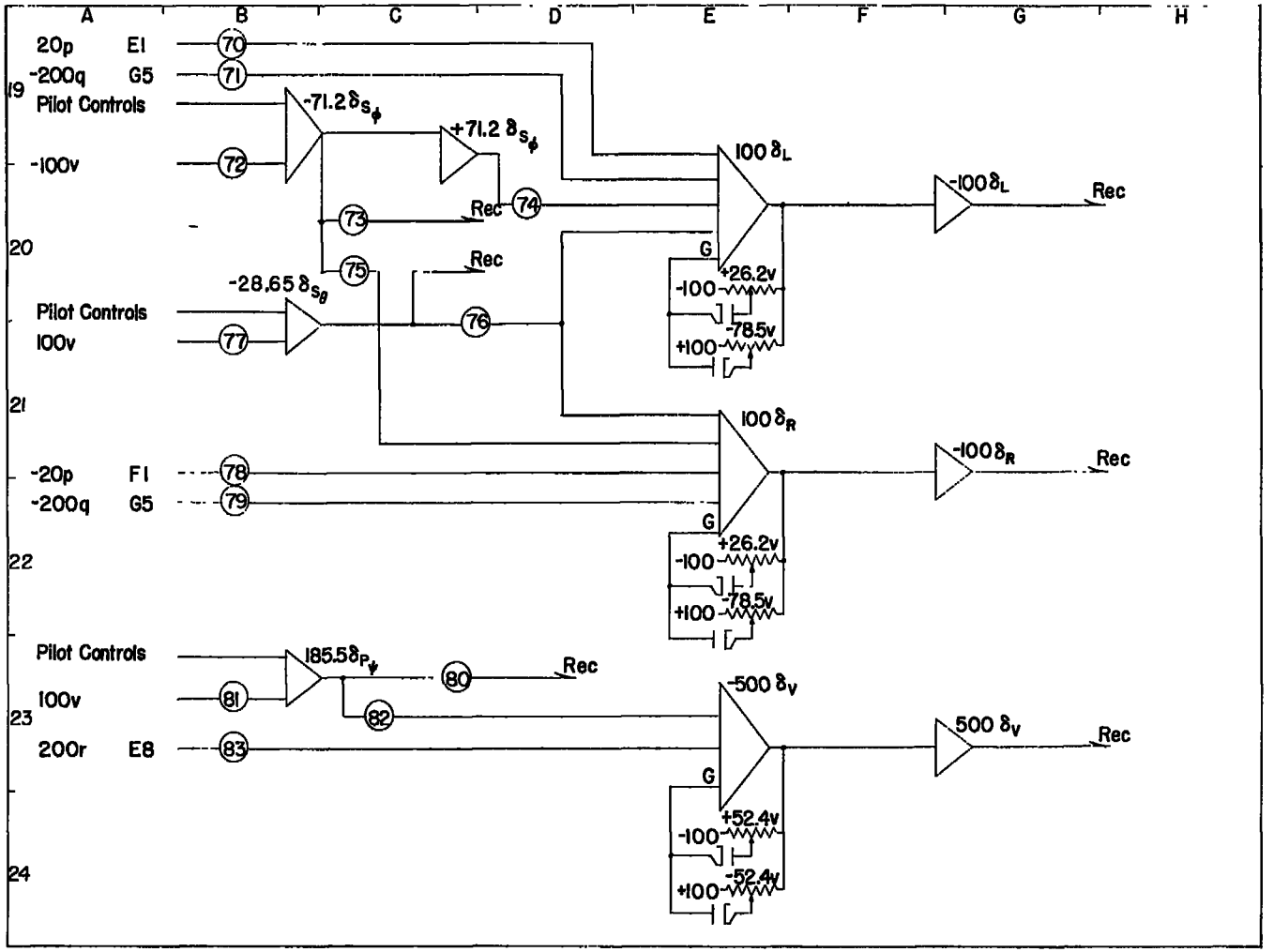

(d) Control circuit.

Figure 12.- Continued.

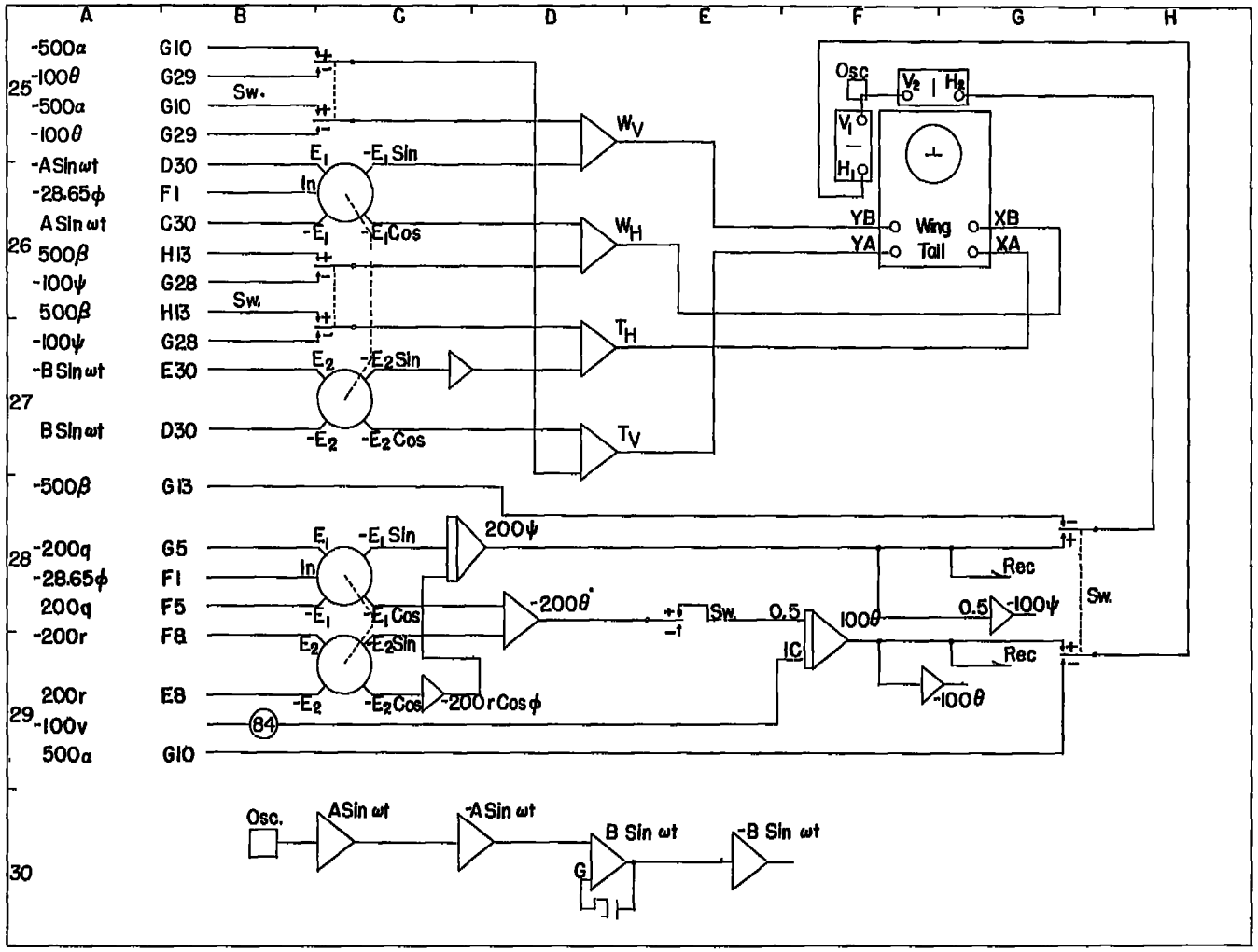

(e) Display circuit.

Figure 12.- Continued.

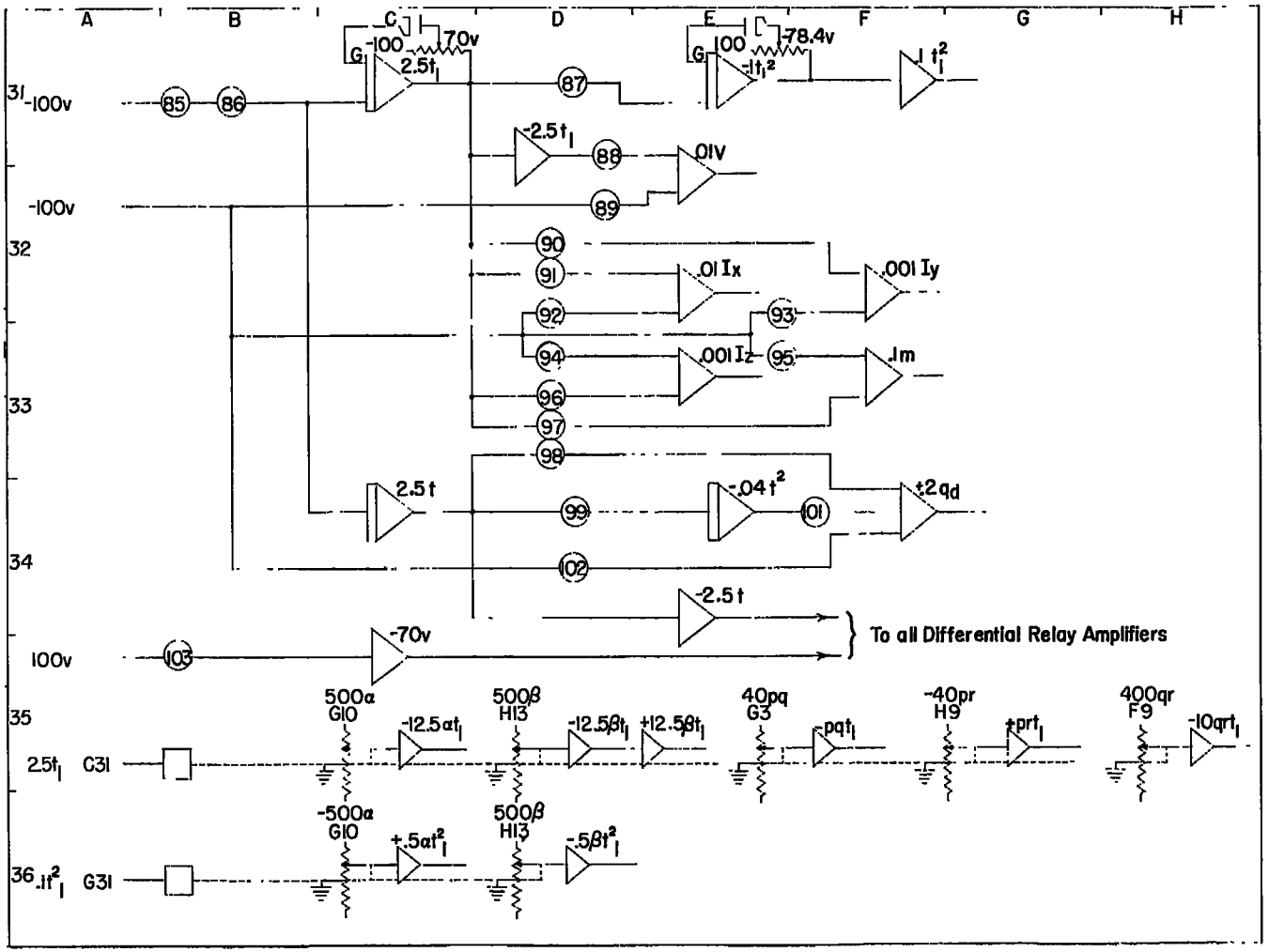

(f) Function generating circuit.

Figure 12.- Concluded.

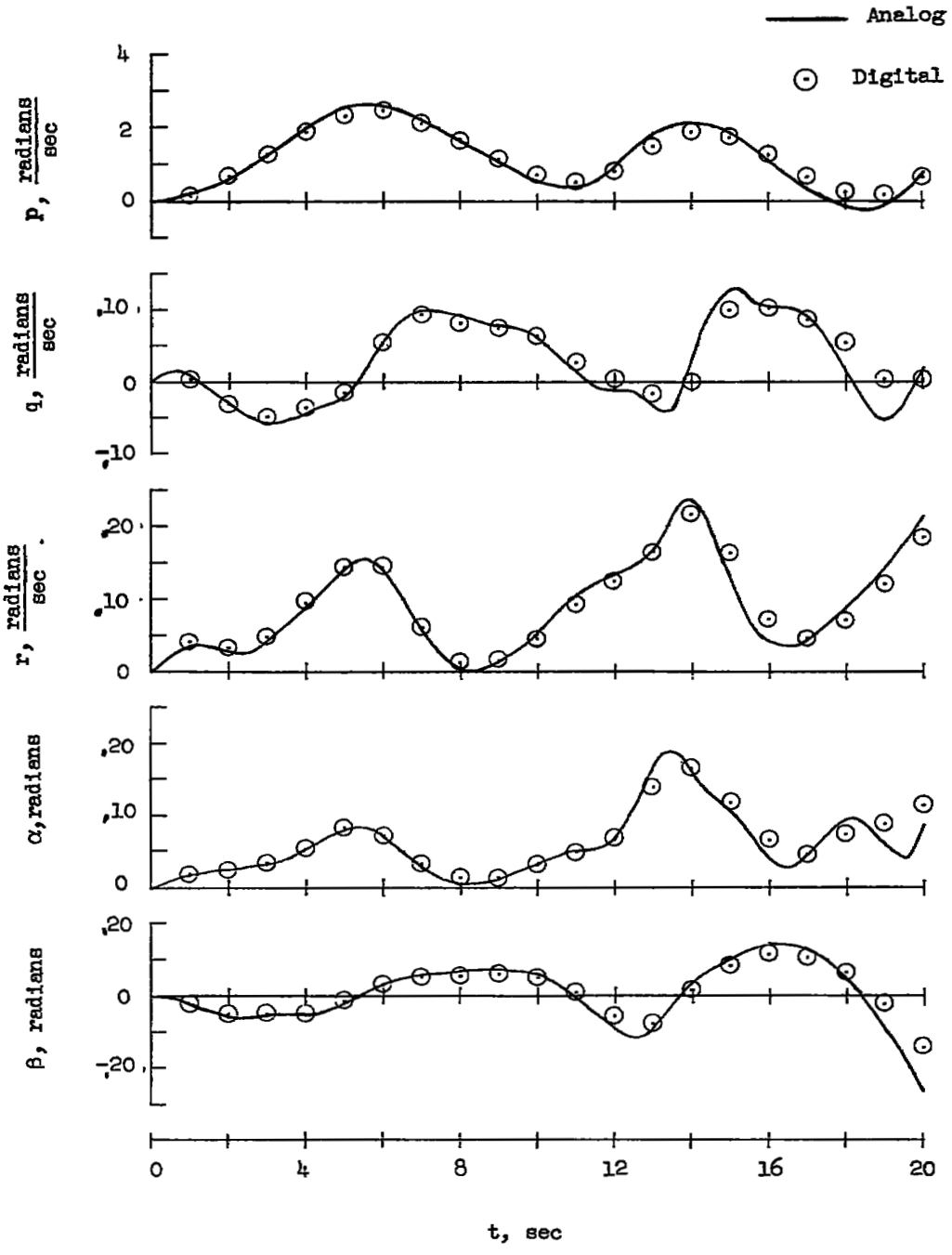

Figure 13.- Comparison of analog computer results with digital check case.